

## 4. CALCAREOUS NANNOFOSSIL BIOSTRATIGRAPHY OF LEG 108 SEDIMENTS<sup>1</sup>

Hélène Manivit<sup>2</sup>

### ABSTRACT

Calcareous nannofossils were examined from the 400 cores recovered at 12 sites during Ocean Drilling Program Leg 108 in the eastern equatorial Atlantic Ocean and along the northwest African margin, representing a transect spanning 24° of latitude.

Thirty calcareous nannofossil biohorizons were recognized in the Neogene and Quaternary sequences; only Site 661, located in water depths of 3500 m, contains a fossiliferous record older than the Oligocene.

At Site 661, a 200-m-thick sequence of Upper Cretaceous sediments yielded Maestrichtian and uppermost Campanian nannofossils, yet a continuous Cretaceous/Tertiary boundary was not recovered. Widespread sediment slumps and turbidites deposited at many sites interrupted the pelagic sedimentation. A careful study of calcareous nannofossil and foraminifer assemblages correlated to paleomagnetic records suggests that "slumped" units at most sites were added as extra sediments to rapidly deposited pelagic sediments, with minor disturbance of the surrounding layers.

Nannofossils are generally common to abundant and moderately preserved at all sites except for those located in two upwelling areas, where placoliths are etched and discoasters overgrown.

Typical low-latitude zonal markers were used during this study, yet some of them were considered to be of little biostratigraphic value because of their inconsistent stratigraphic ranges and low abundances. This is especially apparent for the intervals representing the Miocene/Pliocene and Oligocene/Miocene boundaries.

Characteristic nannofossils of cool-water conditions and low discoaster abundances occur at the coastal African upwelling and along the south equatorial divergence sites, signifying a stronger advection of cold waters toward the equator within the Canary and Benguela eastern boundary currents.

### INTRODUCTION

Leg 108 of the Ocean Drilling Program (ODP) cored 12 sites in the eastern equatorial Atlantic and along the northwest African margin, representing a transect spanning about 24° of latitude (Fig. 1).

Cenozoic sediments were recovered by continuous hydraulic piston coring with the advanced hydraulic piston corer (APC) and the extended core barrel (XCB). Ages of the samples examined range from the late Oligocene (NP23) through the Quaternary (*Emiliania huxleyi* Zone NN21).

Cenozoic sediments generally contain common to abundant, moderately well-preserved nannofossils. Neogene species assemblages are relatively diverse and allow the use of low-latitude zonation. I rarely encountered reworked older taxa except in the slumped sediments of Sites 662, 663, 664, 665, and 666.

### METHODS

The light microscope ( $\times 1200$  magnification) was used to examine the smear slides prepared according to standard procedures. A few selected samples were studied by scanning electron microscope (SEM) to confirm the presence of *Emiliania huxleyi* in cores where it was suspected and to examine the Upper Cretaceous samples in Hole 661A.

An appendix gives the full generic and specific names of all taxa considered in this report. Zonal assignments of the cores from Sites 657 to 668 are summarized in Tables 1 and 2. Figure 2 gives a correlation of Martini (1971) zones with the low-latitude zonation of

Okada and Bukry (1980), which seems more suitable for the Tertiary and Quaternary deep-sea sediments recovered during Leg 108. The age (Ma) of Pleistocene and Pliocene datums are from Backman and Shackleton (1983). For the Cretaceous sediment from Hole 661A, I have employed the same zonal definitions used by Perch-Nielsen (1977), Pflaumann and Čepk (1982), and Stradner and Steinmetz (1984).

Tables 3 through 14 present the abundance, preservation, and stratigraphic distribution of calcareous nannofossils, using code letters as explained below, with the addition of "r" for reworked.

#### Abundance

The abundances of individual species are defined as follows:

Rare: <0.1% (of the total assemblage),  
Few: 0.1%–1.0% (of the total assemblage),  
Common: 1.0%–10.0% (of the total assemblage), and  
Abundant: >10.0% (of the total assemblage).

#### Preservation

Although estimates of preservational states of the nannofossil assemblages reflect a high degree of subjectivism, I used Roth and Thierstein's chart (1972) during Leg 108, modifying the original version in order to adjust to ODP standards (good, moderate, and poor). The placoliths showed characteristic signs of more or less intense dissolution whereas the discoasters commonly displayed varying degrees of overgrowth.

Good = "G" corresponds to an excellent preservation showing no signs of dissolution or overgrowth;

Moderate = "M" corresponds to a slight to moderate dissolution of placoliths and a slight to moderate overgrowth of discoasters. Species are still clearly recognizable.

Poor = "P" is used for severe dissolution of placoliths, abundant broken and/or isolated shields of placoliths, or severe overgrowth of discoasters with strongly thickened arms. The species often are unrecognizable.

<sup>1</sup> Ruddiman, W., Sarnthein, M., et al., 1989. Proc. ODP, Sci. Results, 108 College Station, TX (Ocean Drilling Program).

<sup>2</sup> C.N.R.S.-UA 319, Laboratoire de Stratigraphie des Continents et Océans, Université Paris VI, 4 Place Jussieu, 75230 Paris Cedex, France.

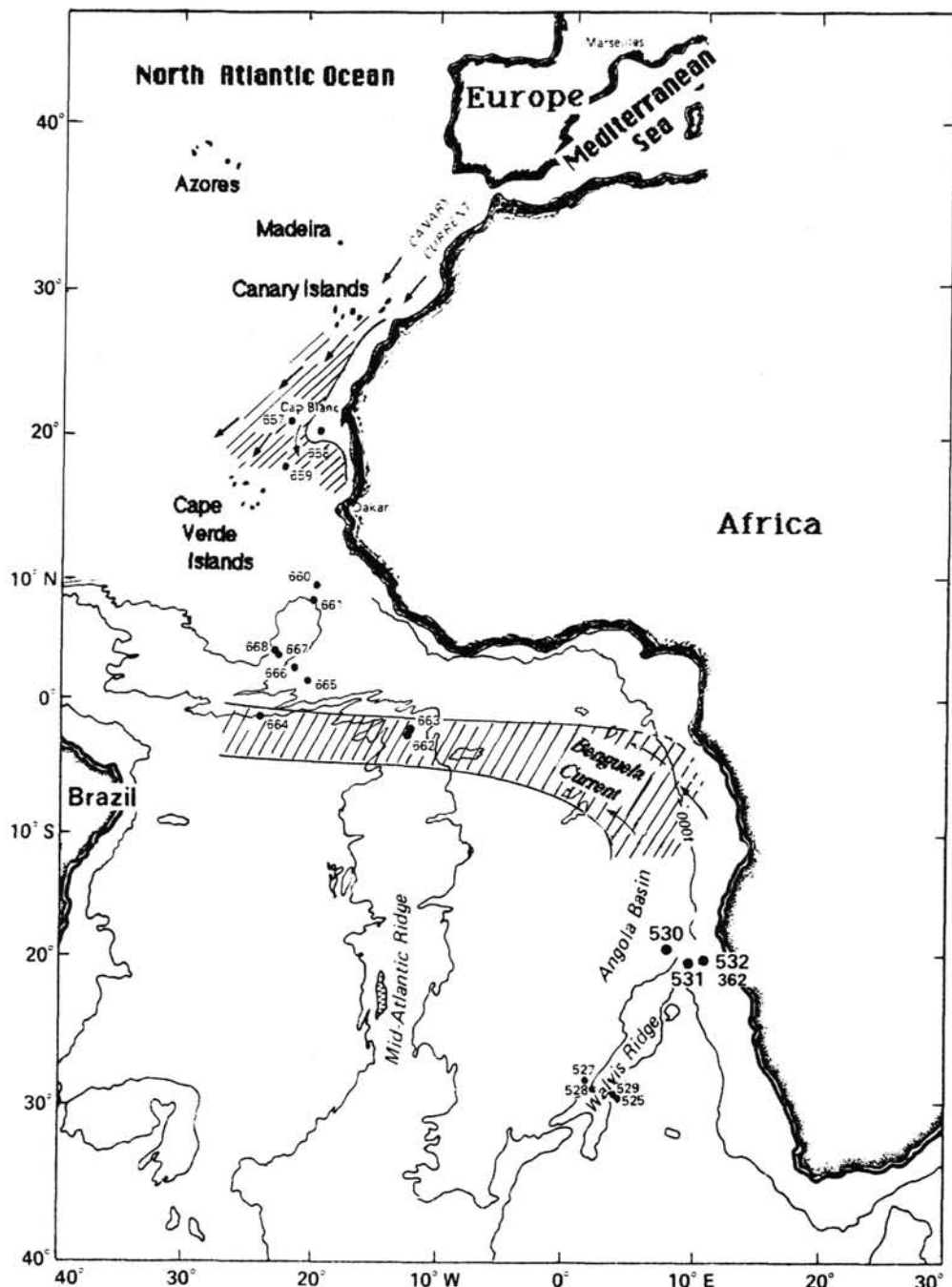


Figure 1. Location map of sites drilled during Leg 108. Arrows mark major current systems, and grey areas indicate regions of strong Pliocene-Pleistocene upwelling and divergence.

## NANNOPLANKTON ZONATION

### Quaternary and Tertiary

The two most well-known zonal schemes for Cenozoic calcareous nannofossils, Martini (1971) and Okada and Bukry (1980), were employed for Leg 108 (Fig. 2). The standard nannoplankton zonation of Martini (1971) was used for the shipboard and site reports. In the range charts (Tables 3–14), Bukry and Okada's (1980) zonal code numbers are indicated.

### Cretaceous

Cretaceous sediments recovered from Hole 661A are Maastrichtian and uppermost Campanian in age (Table 2). The definitions of the zones recognized at Site 661 are discussed below from the bottom of the recovered sections to the top.

The oldest Cretaceous sediments are placed in the *Quadrup. trifidum* Zone Bukry and Bramlette (1970), which is defined as the interval from the first occurrence (FO) to the last occurrence (LO) of *Quadrup. trifidum*. This zone is easily

**Table 1. Geologic age and nannoplankton zone assignment of Leg 108 samples.**

Quaternary		Zones	Hole 657A	Hole 657B	Hole 658A	Hole 658B	Hole 658C	Hole 659A	Hole 659B	Hole 659C	Hole 660A	Hole 660B	Hole 661A
NN21	1H-2, 105	1H-1, 85	1H to 5H-CC	1H to 5H-CC	1H to 7H-CC	1H to 1H-CC	1H to 2H	1H-1, 70 1H-5, 130	1H-6 2H-4, 23	1H-1 to 2H-CC	1H to 3H-3	1H	
NN20	1H-3, 50	1H to 1H-CC	6H to 8H-4, 30	6H to 8H-CC									1H-CC 2H-4, 120
NN19	1H-3, 150 7H-3, 62	2H-1, 59 to 7H-CC	8H-5, 30 14H-3, 145	9H-1, 24 14H-6	8H	2H-1, 30 5H-CC	2H to 6H-6, 3	2H-5, 30 to 4H-CC	3H-4, 23 6H-1, 85	3H-4 5H-2, 130	2H-5, 80 4H-5, 100		
NN18	7H-3, 148 to 8H-1, 5	8H-1, 50 8H-4, 45	14H-5, 145 17H-6, 71	14H-6, 110 18H		7H-1, 5 8H-5, 5	6H-6, 100 8H-4, 20	5H-1	6H-5, 6 6H-5, 140	5H-3, 70 6H-1, 20	4H-6, 80 5H-3, 80		
NN17	8H-5, 10	8H-5, 10 to 9H	17H-CC to 19H-6	18H-CC		8H-6, 5 to 12H-5, 5	8H-5, 20 to 12H-5		6H-6, 140 7H-3, 70	6H-1, 100 6H-2, 20	5H-4, 80 5H-5, 80		
NN16	8H-CC 12H-CC	9H-2, 147 11H-CC	19H-7, 149 to 32H			12H-6, 5 13H-6, 75	12H-6, 50 to 14H	5H-6, 70 to 6H	8H-5, 120 to 9H-3	8H-2, 30 to 9H-2, 14	5H-6, 80 7H-4, 24		
NN15	13H-1, 75 14H-4, 130	12H-1, 40 to 12H	32H-CC			13H-CC to 16H-4	14H to 16H-CC	6H					
NN14	14H-5, 30 to 15H-1	12H to 13H				16H-5, 30 to 16H-CC	17H to 17H-3, 90		9H-3, 55	9H-3, 57 to 9H-4	7H-6, 90 8H-6, 90		
NN13	15H-2, 50 to 15H-4, 129	13H to 16H				17H-CC 20H-3, 75	17H-4, 50 to 20H-CC	7H to 7H-CC	9H-6, 104	9H-5, 100	8H-6, 150 9H-1, 10		
NN12						20H-3, 135 to 21H-3	21H-1, 130 22H-1, 102	8H to 8H-CC					
NN11	15H-5, 40 18H-CC	16H-4, 50 17H-CC				21X-3, 140 22X-1, 75	22H-1, 30 22H-2, 102						
NN10		18H-1, 24 to 19H-CC				22X-1, 134 22X-2, 42	22H-3, 132 22H-4, 120						
NN9						22X-2, 146 23X-3, 140	22H-5, 6						
NN8						23X-4, 114 24X-2							
NN7						24X-CC 25X-2, 125							
NN6						25X-5, 125 to 25X-CC							
NN5						26X-CC to 27X-1							
NN4						27X-1, 140 27X-2							
NN3						27X-3, 34 27X-5, 80							
NN2						27X-6, 138 27X-CC							
NN1													
NP25													
NP24													
NP23													

Table 1 (continued).

Quaternary		Zones	Hole 661B	Hole 662A	Hole 662B	Hole 663A	Hole 663B	Hole 664B	Hole 664C	Hole 664D	Hole 665A	Hole 665B	Hole 666A	Hole 667A	Hole 667B	Hole 668B
		NN21	1H to 2H-5, 110	1H to 2H-1, 86	1H to 3H	1H-1, 110 1H-3, 128	1H to 2H-5	1H-1, 14 1H-5, 120	1H to 2H	1H to 3H	1H to 2H-4, 93	1H to 2H-3, 130	1H to 2H-1, 107	1H to 2H-3, 110	1H to 2H, 1 (top)	1H to 2H-4, 130
		NN20		2H-2, 10 4H-1, 100		1H-4, 128 2H-CC		1H-6, 130 2H-3, 90								
Pliocene	late	NN19	2H-6, 120 4H-1, 100	4H-2, 50 14H-5, 0	3H-CC to 6H	3H-1, 130 12H-3, 40	2H-6, 40 11H-6, 50	2H-4, 100 11H-2, 80	3H to 7H-CC	3H-3, 3 to 8H-CC	2H-5, 60 5H-3, 120	5H-1, 50 6H-1, 110	2H-2, 110	2H-4, 110 to 4H-CC	2H-1, 100 4H-3, 100	2H-5, 130 4H-5, 111
		NN18	4H-2, 145 4H-6, 131	14H-5, 75 17H-1, 75	6H to 9H-CC	12H-3, 100 15H-4, 30	11H-6, 80 14H-7, 10	11H-6, 80 to 12H	12H-3, 58 12H-6, 60	9H-1, 110 12H-2, 58	5H-4, 30 6H-4, 10	6H-2, 20 to 6H	6H-2, 110 8H-2, 45	5H-2, 90	4H-4 to 5H-1, 90	4H-6, 40
		NN17	4H-CC to 5H-1, 60	17H-2, 140 17H-3, 100	10H	15H-5, 80 16H-1, 90	15H-1, 60 16H-1, 60	12H to 12H-6		12H-4, 80	6H-CC to 9H-1	8H-3, 33 8H-4, 80	5H-3, 110 5H-4, 80			
		NN16	5H-2, 130 7H-1, 90	17H-3, 110 22H-1, 70	10H-CC 11H-CC	16H-4, 100 16H-CC	16H-2, 60 to 16H-CC	13H to 19H		12H-CC to 18H-6, 120	6H-5, 90 8H-3, 90			8H-4, 110 to 14H-3	5H-5, 114 7H-1, 50	5H-2, 40 6H-2, 50
		NN15	7H-2, 50 to 7H-4, 100	22M-2, 50 22H-CC	12H			20H to 23H	24H to 25H-CC	18H-CC to 21H	8H-4, 100 to 9H-3, 77			14H-3, 130	7H-1, 135 to 9H-5	6H-3, 100 to 9H-2, 100
	early	NN14								21H to 23H-2, 10				9H-6, 52		
		NN13	7H-5, 90 to 7H-CC							26H				16H-CC	10H-1, 101 10H-5, 86	9H-3, 120 to 10H-CC
		NN12	8H-1, 50 8H-4, 10								26H-2, 10 31H-4, 20				10H-6, 31 14H-2, 78	11H to 13H-6
		NN11	8H-5, 50 9H-4, 100								31H-6, 20 32H-5, 110				14H-3, 120 to 14H-CC	13H-CC to 14H
		NN10	9H-5, 130 to 9H-CC								32H-6, 110 32H-CC					14H-2, 100
Miocene	middle	NN9													17H-4, 100 to 17H-CC	
		NN8													18H-1, 70 18H-5, 50	
		NN7													18H-5, 110 to 22H-CC	
		NN6													23H-CC	
		NN5													24X-CC	
	early	NN4													25X-CC to 35X-CC	
		NN3													36X-CC to 37X-5	
		NN2													37X-5, 137 to 40X-CC	
		NN1													41X-3 to 41X-CC	
		NP25														
Oligocene		NP24														
		NP23														

Note: Core-section interval given in centimeters.

**Table 2. Calcareous nannofossil zonation for Upper Cretaceous sediments from Hole 661A.**

Age	Zone	Core, sample interval (cm)
late Maestrichtian	<i>Micula murus</i>	108-661A-12H-6, 121 108-661A-13H-6, 100
middle Maestrichtian	<i>Arkhangelskiella cymbiformis</i>	108-661A-13H-CC to 108-661A-14H-7, 140
early Maestrichtian		108-661A-14H-8, 84
late Campanian	<i>Quadrum trifidum</i>	108-661A-18X-1, 105 108-661A-18X-2, 100

recognizable in low latitudes and principally in the South Atlantic (Manivit, 1984; Perch-Nielsen, 1977). Its age is upper Campanian to lower Maestrichtian. In this zone, cosmopolitan events such as the FO of *Reinhardtites levis* and the LOs of *Reinhardtites anthophorus* and *Eiffelithus eximius* are used for determining the Campanian/Maestrichtian boundary.

The chronostratigraphic ages for the Campanian/Maestrichtian boundary vary between 75–69 Ma and 71–72.3 Ma with different authors (see the remarks and discussions in Stradner and Steinmetz, 1984, pp. 589–591). Generally, the FO of *Q. trifidum* is calibrated to the middle of Chron 33N and the LO of *Q. trifidum* correlates with the upper portion of Subchron C32N (see the Bottaccione reference section near Gubbio studied by Monechi and Thierstein, 1985).

The LO of *Q. trifidum* marks the base of the *Arkhangelskiella cymbiformis* Zone, which is defined as the interval from the LO of *Q. trifidum* to the FO of *Lithraphidites quadratus*. In Hole 661A, only the lower proportion of the *A. cymbiformis* Zone can be determined, as at Deep Sea Drilling Project (DSDP) Site 530 in the Angola Basin (Stradner and Steinmetz, 1984). The lack of the taxon *L. quadratus* in these sites does not seem attributable to ecologic conditions but, rather, to the poor preservation of nannofossils in the Maestrichtian sediments.

The FO of *Micula murus* indicates the upper boundary of the *A. cymbiformis* Zone and the base of the *M. murus* Zone. Depending on the time scale that is used, the approximate duration of the *M. murus* Zone falls between about 66.7 and 68.6 Ma, correlating to Chron 30 and the upper part of Chron 31 (see Manivit, 1984, and Monechi and Thierstein, 1985).

At Site 661 the uppermost Maestrichtian zonal marker *Micula prinsii* was observed over about 1 m; it was rare to few in this interval, which contains several coccoliths and only rare *Thoracosphaera* fragments. At Sites 525, 527, 528, and 530 (Manivit, 1984; Steinmetz and Stradner, 1984), the *M. prinsii* Zone was generally limited to the uppermost 1–1.5 m below the Cretaceous/Tertiary boundary and showed an increasing abundance of *Thoracosphaera* specimens.

## SUMMARY OF NANNOFOSSIL BIOSTRATIGRAPHY

### Site 657

Two holes were drilled at the “nonupwelling” site off the shore of northwest Africa. Water depths of 4231 m have resulted in the considerable dissolution of carbonate.

Calcareous nannofossils are abundant in all the samples examined from the Pliocene and Pleistocene sediments recovered from Holes 657A and 657B (Table 3). Both the placolith and discoaster assemblages show slight to moderate etching in the Pliocene-Pleistocene sequence. In the upper Miocene

sequence, the assemblages mainly consist of discoasters and ceratoliths, which show neither dissolution nor overgrowth. Placoliths are severely dissolved. The brownish and greenish clays of the late Miocene are barren of calcareous nannofossils in some intervals.

The sediments range in age from Pleistocene to late Miocene (8.2 and 8.5 Ma). Reworking of calcareous nannofossils at Site 657 is negligible, but downhole displacement of sediment was confirmed in several core-catcher samples.

### Holocene

On board, SEM studies showed that the reversal in dominance between *Emiliana huxleyi* and *Gephyrocapsa* spp. could be located between Samples 108-657A-1H-2, 5 cm, and 108-657A-1H-2, 105 cm, which suggests an age of 0.09 Ma for this event.

### Pleistocene

The Pleistocene assemblages are dominated by *Gephyrocapsa* spp.; I have made no attempt in this report to separate them at the species level. The other typical nannofossils are *Coccolithus pelagicus*, *Calcidiscus leptoporus*, *Helicopontosphaera kampfneri*, *Pontosphaera japonica*, *Syracospaera* spp., *Rhabdosphaera* spp., and occasionally rare *Scyphosphaera* spp. and *Ceratolithus cristatus*. In the lower Pleistocene, the assemblages contain rare to few *Helicopontosphaera sellii* and common *Calcidiscus macintyrei*. Section 108-657A-4H-CC contains very abundant, small *Gephyrocapsa* spp. and may represent the “small *Gephyrocapsa acme* Zone” of Gartner (1977).

### Pliocene

The LO of *Discoaster brouweri* is accompanied by that of *Discoaster triradiatus* in both holes and by a decreasing dominance of gephyrocapsids at about 1.9 Ma, whereas the small reticulofenestrids constitute the major assemblage element down the basal Pliocene. In Section 108-657B-16H-CC, the specimens of *Reticulofenestra minuta* dominate all other assemblage components. Within Cores 108-657A-14H and 108-657B-12H the extinction of amaurolithids, including *Amaurolithus tricorniculatus*, marks the top of Zone NN14.

I did not determine the base of this zone because of the low abundance of the marker species *Discoaster asymmetricus* near the beginning of its range. *Ceratolithus rugosus* are few in Core 108-657A-15H and are generally poorly preserved with much secondary overgrowth. The evolutionary transition from *Ceratolithus acutus* to *Ceratolithus rugosus* was tentatively recognized in the upper part of Section 108-657A-15H-4, where I placed the approximate location of the NN12/NN13 zonal boundary.

### Miocene

The FO of *Ceratolithus acutus*, characteristic of basal Zone NN12 is in Sample 108-657A-15H-4, 130 cm. However, Zone NN12, which has a current duration of 1 m.y. (4.6–5.6 Ma), is only represented in Hole 657A by 1.5 m of sediment (from upper Section 108-657A-15H-4 to upper Section 108-657A-15H-5). Therefore, the Miocene/Pliocene boundary seems to be missing. In Hole 657B, a hiatus spanning this interval occurs between Sample 108-657B-16H-4, 50 cm (NN11), and Sample 108-657B-15H-CC (NN12/NN13). *Amaurolithus amplificus*, which disappears in Sample 108-657A-16H-5, 0 cm, shows a diachronic extinction with that of *D. quinqueramus* (Sample 108-657A-15H-5, 40 cm). This discoaster continues its range at least 6 m above the LO of *A. amplificus*.

Age		Zone and subzone			Datum	Age (Ma.)
		(1)	(2)		(2)	
Quaternary		NN21	CN15	<i>Emiliania huxleyi</i>	—	Increase <i>Emiliania huxleyi</i> 0.09
		NN20	CN14	<i>Gephyrocapsa oceanica</i>	CN14b	FO <i>Emiliania huxleyi</i> 0.28
		NN19	CN13	<i>Pseudoemiliania lacunosa</i>	CN14a CN13b CN13a	LO <i>P. lacunosa</i> 0.47 FO <i>G. oceanica</i> , LO <i>H. sellii</i> 1.37 LO <i>C. macintyreai</i> 1.45 FO <i>G. caribbeanica</i> 1.70
	Pliocene	NN18			CN12d	LO <i>D. brouweri</i> LO <i>D. triradiatus</i> 1.89
		NN17	CN12	<i>Discoaster brouweri</i>	CN12c	Increase <i>D. triradiatus</i> 2.07
		NN16			CN12b CN12a	LO <i>D. pentaradiatus</i> 2.35 LO <i>D. surculus</i> 2.41 LO <i>D. tamalis</i> 2.65
Miocene	middle	NN15	CN11	<i>Reticulofenestra pseudoumbilica</i>	CN11b CN11a	LO <i>Sphenolithus spp.</i> 3.45 LO <i>R. pseudoumbilica</i> 3.56
		NN14			CN10c	Acme <i>D. asymmetricus</i>
		NN13	CN10	<i>Amaurolithus tricorniculatus</i>	CN10b CN10a	LO <i>A. tricorniculatus</i> 3.7 LO <i>Amaurolithus primus</i> 4.4
		NN12				FO <i>C. rugosus</i> , LO <i>C. acutus</i> 4.6
		NN11	CN9	<i>Discoaster Quinqueramus</i>	CN9b CN9a	FO <i>C. acutus</i> , LO <i>T. rugosus</i> 5.0
		NN10	CN8	<i>Discoaster neohamatus</i>	CN8b CN8a	LO <i>D. quinqueramus</i> 5.6 FO <i>A. primus</i> 6.5
	early	NN9	CN7	<i>Discoaster hamatus</i>	CN7b CN7a	FO <i>D. berggrenii</i> 8.2 FO <i>D. quinqueramus</i>
		NN8	CN6	<i>Catinaster coalitus</i>	—	FO <i>D. neorectus</i> , <i>D. loeblichii</i> 8.5
		NN7	CN5	<i>Discoaster exilis</i>	CN5b CN5a	LO <i>D. hamatus</i> 8.85
		NN6				FO <i>C. calyculus</i> 9.8
		NN5	CN4	<i>Sphenolithus heteromorphus</i>	—	FO <i>D. hamatus</i> 10.0
		NN4	CN3	<i>Helicosphaera ampliaperta</i>	—	FO <i>C. coalitus</i> 10.8
Oligocene		NN3	CN2	<i>Sphenolithus belemnos</i>	—	LO <i>C. floridanus</i> FO <i>D. klugeri</i> 13.5
		NN2		<i>Triquetrorhabdulus carinatus</i>	CN1c CN1b CN1a	LO <i>S. heteromorphus</i> 14.4
		NN1	CN1		CP19b CP19a	FO <i>C. macintyreai</i> , LO <i>H. ampliaperta</i> 16.8
		NP25	CP19	<i>Sphenolithus ciperoensis</i>	CP19b CP19a	FO <i>S. belemnos</i> , LO <i>T. carinatus</i> 21.5
		NP24	CP18	<i>Sphenolithus distentus</i>	—	FO <i>D. druggii</i> 23.2
		NP23	CP17	<i>Sphenolithus predistentus</i>	—	Acme <i>C. abiseptus</i> 23.7
						LO's <i>D. bisectus</i> , <i>H. recta</i> , <i>S. ciperoensis</i> 25.2
						LO <i>S. distentus</i> 28.2
						LO <i>S. ciperoensis</i> 30.2
						FO <i>S. distentus</i> LO <i>H. compacta</i> 34.2

Figure 2. Nannofossil zonation scheme used in this chapter. Sources of data are (1) Martini, 1971, and (2) Okada and Bukry, 1980; ages are after Backman and Shackleton, 1983. FO = first occurrence and LO = last occurrence.

### Site 658

Three holes were cored at this site, which is located in an area of intense upwelling off the shore of Cap Blanc in 2263 m water depth. The sediments range in age from early Pliocene through Holocene. The Pleistocene sequence above the LO of *Pseudoemiliania lacunosa* contains well-preserved calcareous nannofossil assemblages (Table 4). Going downhole, the early Pleistocene and Pliocene assemblages become progressively more dissolved and the deepest cores contain etched planoliths and overgrown discoasters.

Nannofossil assemblages at this site were probably controlled by a depositional environment characterized by high productivity from upwelling and entailing diagenetic consequences. Although Site 658 was located at latitude 20°N, the Pliocene discoasters show exceptionally low relative abundances, hardly contributing more than 1% of the total assemblage. This low abundance is typical for the northernmost North Atlantic rather than for tropical areas.

### Pleistocene

The Pleistocene sequence at Site 658 is completely dominated by gephyrocapsids. Common assemblage elements consist of *Calcidiscus leptoporus*, *Coccolithus pelagicus*, and *Helicosphaera carteri*. Shortly below Cores 108-658A-8H and -9H, a marked increase in the etching of nannofossil assemblages was observed in both holes. *Calcidiscus macintyreai* and *Helicosphaera sellii* last occur very close to each other between Samples 108-658A-11H-6, 35 cm, and 108-658A-11H-6, 65 cm. This suggests the existence of a small hiatus at a depth of 99 m below seafloor (mbsf) since the LOs of these two species are known to differ.

### Pliocene

Coccolith species diversity is good in the three holes cored at Site 658. The Pliocene assemblages are fairly uniform, with abundant small reticulofenestrids. Rhabdosphaerids and discoasters are rare. Because of the low abundances of the

Table 3. Distribution of Pleistocene to late Miocene calcareous nannofossils, Hole 657A.

Age	Zonation		Preservation	Abundance	Core, section, interval (cm)		
	Okada and Bukry, 1980	Martini, 1971					
Pleistocene	CN15	NN21	G A	1H-2, 5-6	Sphenolithus abies/neobabis		
	CN14b	NN20	G A	1H-2, 105-106	Ceratolithus acutus		
		M A	1H-3, 50-51		Amaurolitus amplificus		
		M A	1H-3, 150-151		Oolithus antillarum		
		M A	1H-CC		Discosaster asymmetricus		
		M C	2H-CC		Discosaster brouweri		
		M A	3H-CC		Gephyrocapsa caribeanica		
		M A	4H-CC		Discosaster challengerii		
		G A	5H-4, 120-121		Rhabdosphaera clavigera		
		G A	5H-5, 120-121		Ceratolithus cristatus		
Pliocene	CN14a	NN19	F		Amaurolitus delicatus		
	CNB13b		R		Syracosphaera hystrica		
		R	R		Emiliania huxleyi		
		R	R		Discosaster intercalis		
		R	R		Pontosphaera japonica		
		R	R		Helicosphaera kampinieri		
		R	R		Pseudomiliaria lacunosa		
		R	R		Calcidiscus leptoporus		
		R	R		Calcidiscus macintyrei		
	CN13a		R		Umbilicosphaera mirabilis		
Miocene	CN12d	NN18	M A	7H-3, 148-149	Gephyrocapsa oceanica		
		M A	7H-4, 5-6		Coccolithus pelagicus		
		M A	7H-4, 150-151		Discosaster pentadeltoides		
		M A	7H-CC		Amaurolitus primus		
		M M	8H-1, 5-6		Dicyccocites productus		
		M A	8H-5, 10-11		Reticulofenestra pseudumbilicalis		
		M A	8H-CC		Scyphosphaera pulcherrima		
		G A	9H-3, 71-72		Syracosphaera pulchra		
		G A	9H-4, 148-149		Discosaster quinqueramus		
		G A	9H-CC		Cycloolithella rotula		
late	CN12c	NN17	R		Ceratolithus rugosus		
	CN12b	NN16	R		Triquerorhabdulus rugosus		
		R	R		Helicosphaera sellii		
		F	C		Umbilicosphaera sibogae		
		F	C		Reticulofenestra "small"		
		C	C		Gephyrocapsa spp.		
		C	C		Thoracosphaera sp.		
		F	F		Rhabdosphaera stylifer		
		F	F		Discosaster sarculus		
	CN12a		R		Discosaster tamalis		
early	CN11	NN15	M A	13H-1, 75-76	Ceratolithus telesinus		
		M A	13H-CC		Amaurolitus tricorniculatus		
		M A	14H-4, 130-131		Discosaster triradiatus		
		M A	14H-5, 30-31		Discosaster variabilis		
		M A	14H-CC				
		M A	15H-2, 50-51				
		M A	15H-4, 129-130				
	CN10c	NN14	R				
	CN10a-b	NN13/12	F R				
late	CN9b	NN11	M A	15H-5, 40-41			
		M A	15H-CC				
		M C	16H-2, 25-26				
		M C	16H-5, 1-2				
		M C	16H-6, 90-91				
		P F	16H-6, 110-111				
		F	16H-CC				
		M F	17H-CC				
		M F	18H-CC				
	CN9a		F				

discoasters in Core 108-658A-16H, it is impossible to determine by counting the increase of *Discoaster triradiatus* (relative to *Discoaster brouweri*) to better than 6 m between Section 108-658A-15H-CC and Sample 108-658A-16H-4, 150 cm.

The extinction of *Discoaster pentaradiatus* is episodic during the interval from Sample 108-658A-17H-CC to Sample 108-658A-19X-7, 149 cm. Moreover, this discoaster shows a less clear abundance as compared with *Discoaster surculus*. The rare occurrence of *Discoaster tamalis* in the lower half of Core 108-658A-22X and in the upper half of Core 108-658A-23X makes the precise identification of the top of Subzone CN12b difficult. Recovery in Core 108-658A-32X was so poor that a precise determination of the LO of *Reticulofenestra pseudoumbilica* (281.4–290.9 mbsf) was difficult, and therefore the top of Zone NN15 was undefinable.

### Site 659

Site 659 is situated on the top of the Cape Verde Rise in a “nonupwelling” region but under the distal Canary Current in a water depth of 3070 m. Three holes were cored. Nannofossils are abundant and well preserved throughout the Pleistocene and most of the Pliocene (Table 4). In general, the abundance and preservation of Miocene placoliths vary as a function of lithology: the bluish clays of the middle and lower Miocene contain severely dissolved placoliths, whereas the white nannofossil oozes of the uppermost Miocene show fewer dissolved assemblages. Miocene discoasters are generally well preserved, with the exception of overgrowths in the lower Miocene *Discoaster deflandrei* assemblages.

#### Pleistocene

The Pleistocene assemblages of Sites 659 are virtually identical with those of Sites 657 and 658.

#### Pliocene

The Pliocene assemblages are generally more diverse than those of the Pleistocene, and the dominant group is the small reticulofenestrids. Toward the basal Pliocene and the uppermost Miocene, the very small species *Reticulofenestra minuta* shows distinct blooms that represent the sum of all other taxa.

An investigation of Core 108-659C-5H suggests that sphenoliths (*Sphenolithus abies* and *Sphenolithus neoabies*) continued to exist 1.6–3.9 m above the range of *Reticulofenestra pseudoumbilica*, which gives an average sedimentation rate of 30 m/m.y. and corresponds to a time interval from about 0.05 to 0.13 Ma. Rare to few amaurolithids occur at Site 659. Because of this, they are of restricted biostratigraphic value. As a consequence, the recognition of the boundary between Zones NN14 and NN15 involves a high degree of uncertainty. At Hole 659A, because *Ceratolithus rugosus*, the FO of which defines the base of Zone NN13, is rare and exhibits specimens that are severely overgrown, it is difficult to place the NN12/NN13 boundary accurately.

#### Miocene

A complete middle and upper Miocene sequence was cored at Site 659. Most of the lower Miocene is represented by a hiatus spanning the interval from upper NN3 (21.5 Ma) to basal NN2 (17 Ma). The Oligocene/Miocene boundary was recognized in the lowermost part of Hole 659A. Hole 659H was cored to approximately the middle/upper Miocene boundary. Two cores of Hole 659C represent the upper Miocene. Discoasters are abundant throughout the Miocene sediments. Placolith assemblages are dominated by reticulofenestrids in the middle and upper Miocene and by *Cyclicargolithus floridanus* in the lower Miocene.

*Amaurolithus amplificus* and *Amaurolithus delicatus* are the most common amaurolithid species in Core 108-659H-19H, although they must be considered rare to few in relation to the total assemblage. All the discoasters and typical Miocene events were recognized in Hole 659A, allowing a good biostratigraphic control (Table 5). Numerous intermediate forms between *D. quinqueramus* and *Discoaster berggrenii* were observed in the lower part of the range of *D. quinqueramus*, but these two morphotypes are not separated here.

Rare *Helicosphaera ampliaperta* were observed in Sample 108-659A-25X-5, 130 cm. Because this species was rare in the open-ocean environment, its absence in Core 108-659A-24X and most of Core 108-659A-25X does not necessarily imply that most of Zone NN4 is missing. The presence of *Dictyococcites bisectus* and *Triquetrorhabdulus carinatus* in Sample 108-659A-27X-6, 138 cm, suggests the uppermost Oligocene age. The absence of *D. bisectus* in Sample 108-659A-27X-5, 80 cm, and above this sample indicates that the Oligocene/Miocene boundary can be located in the lower portion of Core 108-659A-27X.

### Site 660

Two holes were drilled at Site 660, which constituted part of a depth transect on the eastern flank of the Kane Gap and is located in water depths of 4332 m. The sediments are middle Eocene and late Miocene to Holocene in age. Nannofossil preservation is good in the upper Pleistocene, moderate in the middle Pleistocene, and poor in the Pliocene and upper Miocene. Severe etching of the coccolith assemblages is observed in the Pliocene and Miocene samples. Discoasters, especially *Discoaster brouweri* and *Discoaster pentaradiatus*, are common in the Pliocene and suggest a warm-water environment during deposition. Discoasters are usually well preserved, although occasional fragments occur. The nannofossil assemblages are very similar to those observed at Site 659.

#### Pleistocene

The absence of *Emiliania huxleyi* in Core 108-660A-1H investigated with the SEM assigned this sample to Zone NN20 (CN14b).

#### Pliocene

The coccolith assemblages are similar in composition throughout the Pliocene and the extinctions of discoasters are easily recognizable (Table 6). Amaurolithids, observed up to Section 108-660A-9H-1, show a bad preservation and low abundance, making it difficult to determine their level of extinction.

#### Miocene

Upper Zone NN11 was recognized in Samples 108-660A-9H-6, 65 cm, and 108-660B-9H-2, 100 cm, due to the co-occurrence of *D. quinqueramus* and amaurolithids. Samples examined stratigraphically below Samples 108-660A-9H-6, 106 cm, and 108-660B-9H-3 are barren of coccoliths.

### Site 661

Two holes were cored at Site 661, situated along the eastern slope of Kane Gap under surface waters of relatively high productivity at 4012.7 m water depth. The oldest Cenozoic sediments at Site 661 were assigned to Zone NN9 and an age of about 9 Ma. The recovery of nannofossil-bearing sediment of Late Cretaceous age (Maestrichtian and latest Campanian) in Hole 661A between 106 and 163 mbsf was very surprising.

**Table 4.** Distribution of Pleistocene to early Pliocene calcareous nannofossils, Hole 658A.

**Table 5.** Distribution of Pliocene to late Oligocene calcareous nannofossils, Hole 659A.

CALCAREOUS NANNOFOSSIL BIOSTRATIGRAPHY

early Pliocene																		
CN11	NN15	M	A	12H-6, 5-6	R		R	F		F		R		C		C		
		M	A	12H-CC	F		F	R		F		R		C		C		
		M	A	13H-1, 15-16	F		R	R		C		R		C		C		
		M	A	13H-2, 75-76	R		R	R		F		R		C		C		
		M	A	13H-3, 75-76	R		R	R		C		R		C		C		
		M	A	13H-6, 75-76	F		R	R		F		R		C		C		
		M	A	13H-CC	F		R	R		F		R		C		C		
		M	A	14H-3, 5-6	F		R	R		F		R		C		C		
		M	A	14H-4, 5-6	F		R	R		F		R		C		C		
		M	A	14H-5, 5-6	F		R	R		F		R		C		C		
CN10c	NN14/13	M	A	14H-CC	F		R	R		F		R		C		C		
		M	A	15H-4, 110-111	F		R	R		F		R		C		C		
		M	A	15H-CC	F		R	R		C		R		C		C		
		M	A	16H-2, 80-81	F		R	R		F		R		C		C		
		M	A	16H-4, 80-81	F		R	R		F		R		C		C		
		M	A	16H-5, 80-81	C	R	R	R		F		R		C		C		
		M	A	16H-6, 44-45	F	R	R	R		F		R		C		C		
		M	A	16H-CC	C	R	R	R		F		R		C		C		
		M	A	17H-CC	C		R	R		F		R		C		C		
		M	A	20H-1, 146-147	F		R	R		R		R		C		C		
CN10a-b	NN12	M	A	20H-3, 75-76	F		R	R		R		R		C		C		
		M	A	20H-3, 135-136	F		R	R		R		R		C		C		
		M	A	20H-CC	C		R	R		R		R		C		C		
		M	A	21X-3, 140-141	F		R	R		R		R		C		C		
		M	A	17H-CC	C		R	R		R		R		C		C		
		M	A	20H-1, 146-147	F		R	R		R		R		C		C		
		M	A	20H-3, 75-76	F		R	R		R		R		C		C		
		M	A	20H-3, 135-136	F		R	R		R		R		C		C		
		M	A	20H-CC	C		R	R		R		R		C		C		
		M	A	21X-3, 140-141	F		R	R		R		R		C		C		
late Miocene																		
middle Miocene																		
early Oligocene																		
CN7 CN6	NN9 NN8	M	C	21X-CC	F		R		F		R		F		F		R	
		M	C	22X-1, 134-135	F		R		F		R		F		F		R	
		M	C	22X-2, 145-146	F		R		F		R		F		F		R	
		M	A	22X-3, 75-76	F		R		F		R		F		F		R	
		M	A	22X-5, 145-146	C		R		F		R		F		F		R	
		M	A	22X-CC	C		R		F		R		F		F		R	
		M	A	23X-3, 140-141	C		R		F		R		F		F		R	
		M	A	23X-4, 114-115	F		R		F		R		F		F		R	
		M	C	23X-5, 110-111	F		R		F		R		F		F		R	
		M	F	23X-CC	C		R		F		R		F		F		R	
CN5b	NN7	M	C	24X-2, 22-23	C		R		F		R		F		F		R	
		M	A	24X-CC	C		R		F		R		F		F		R	
		M	A	25X-2, 125-126	F		R		F		R		F		F		R	
		M	A	25X-5, 130-131	F	R	R		F		R		F		F		R	
		M	C	25X-CC	R	R			F		R		F		F		R	
		P	C	26X-CC	F				F		R		F		F		R	
		P	C	27X-1, 140-141	R				F		R		F		F		R	
		M	A	27X-3, 34-35	A				R		R		R		A		C	
		M	A	27X-6, 137-138	A				F		R		F		A		C	
		M	A	27X-CC	A				C		R		C		A		C	
Oligocene	CN1b-c	NN1	M	A	27X-3, 34-35	A			R		R		R		A		C	
	CP19	NP25	M	M	A	27X-6, 137-138	A		F		R		R		A		C	
			M	M	A	27X-CC	A		C		R		C		F		R	

**Table 5 (continued).**

early Pliocene	CN11	NN15	M A 12H-6, 5–6	R	F	F			R	F	R	R	R	A	R	R	R	R	R	R
			M A 12H-CC	R	R	C			R	F	R	R	R	A	R	R	R	R	R	R
			M A 13H-1, 15–16	F	R	C			R	F	R	R	R	A	R	R	R	R	R	R
CN10c	NN14/13		M A 13H-2, 75–76	R	F	F			R	F	R	R	R	A	R	R	R	R	R	R
			M A 13H-3, 75–76	F	R	F			R	F	F	R	R	A	R	R	R	R	R	R
			M A 13H-6, 75–76	F	R	F			R	F	F	R	R	A	R	R	R	R	R	R
CN10a-b	NN12		M A 13H-CC	R	R	C			R	F	F	R	R	A	R	R	R	R	R	R
			M A 14H-3, 5–6	R	R	C			R	F	F	R	R	A	R	R	R	R	R	R
			M A 14H-4, 5–6	F	R	C			R	F	F	R	R	A	R	R	R	R	R	R
late	CN9b CN9a	NN11	M A 14H-5, 5–6	F	R	C			R	F	F	R	R	A	R	R	R	R	R	R
			M A 14H-CC	R	R	C			R	F	F	R	R	A	R	R	R	R	R	R
			M A 15H-1, 110–111	F	R	C			R	F	F	R	R	A	R	R	R	R	R	R
CN8b CN8a	NN10		M A 15H-CC	F	R	C			R	F	F	R	R	A	R	R	R	R	R	R
			M A 16H-2, 80–81	F	R	F			R	F	F	R	R	A	R	R	R	R	R	R
			M A 16H-4, 80–81	R	F	C			R	F	F	R	R	A	R	R	R	R	R	R
Miocene middle	CN7 CN6	NN9 NN8	M A 16H-5, 80–81	F	R	C			R	F	F	R	R	A	R	R	R	R	R	R
			M A 16H-6, 44–45	R	F	C			R	F	F	R	R	A	R	R	R	R	R	R
			M A 16H-CC	F	R	F			R	F	F	R	R	A	R	R	R	R	R	R
CN5b	NN7		M A 20H-1, 146–147	F	F	F			R	F	F	R	R	A	R	R	R	R	R	R
			M A 20H-3, 75–76	C	F	F			R	F	F	R	R	A	R	R	R	R	R	R
			M A 20H-3, 135–136	F	F	F			R	F	F	R	R	A	R	R	R	R	R	R
CN5a	NN6		M A 20H-CC	F	F	R			R	F	F	R	R	A	R	R	R	R	R	R
			M A 21X-3, 140–141	F	F	R			R	F	F	R	R	A	R	R	R	R	R	R
			M A 21X-CC	F	F	R			R	F	F	R	R	A	R	R	R	R	R	R
CN4	NN5		M C 22X-1, 134–135	F	R	R			R	F	F	R	R	A	R	R	R	R	R	R
			M C 22X-2, 145–146	F	R	R			R	F	F	R	R	A	R	R	R	R	R	R
			M A 22X-3, 75–76	R	C	R			R	F	F	R	R	A	R	R	R	R	R	R
early	CN3 CN2 CN1a	NN4 NN3 NN2	M A 22X-5, 145–146	R	C	R			R	F	F	R	R	A	R	R	R	R	R	R
			M A 22X-CC	F	R	R			R	F	F	R	R	A	R	R	R	R	R	R
			M A 23X-3, 140–141	R	C	R			R	F	F	R	R	A	R	R	R	R	R	R
Oligo- cene	CN1b-c CP19	NN1 NP25	M A 23X-4, 114–115	R	R	R			R	F	F	R	R	A	R	R	R	R	R	R
			M C 23X-5, 110–111	M	F	R			R	F	F	R	R	A	R	R	R	R	R	R
			M C 23X-CC	M	C	R			R	F	F	R	R	A	R	R	R	R	R	R
			M C 24X-2, 22–23	M	C	R			R	F	F	R	R	A	R	R	R	R	R	R
			M A 24X-CC	M	A	R			R	F	F	R	R	A	R	R	R	R	R	R
			M A 25X-2, 125–126	M	A	R			R	F	F	R	R	A	R	R	R	R	R	R

**Table 6. Distribution of Pleistocene to late Pliocene calcareous nannofossils, Hole 660A.**

Preservation improves in sediments of early Pleistocene and late Pliocene age, but it is preceded by increased dissolution of the lower Pliocene assemblages and severe dissolution of the upper Miocene assemblages. The Upper Cretaceous assemblages are all poorly preserved, displaying large amounts of fragmented placolith rims with dissolved central areas.

#### Pleistocene

The Pleistocene sediments alternate between dark muds barren of nannofossils and yellowish oozes showing poorly preserved assemblages. The late Pleistocene (Zone CN15) is not present in Site 661 since neither *Emiliania huxleyi* nor abundant gephyrocapsids were identified.

Late Pliocene discoasters showing high abundances and no reworking provide good biostratigraphic control at Site 661 (Table 7). The most abundant coccoliths are small placoliths (<4 µm), belonging either to *Gephyrocapsa* or *Reticulofenestra*, species only differentiable by SEM observation.

#### Miocene

The Miocene assemblages are characterized by well-preserved discoasters and poorly preserved placoliths reduced to the more dissolution-resistant forms. Reticulofenestrid species dominate the placoliths. Cenozoic nannofossils were not observed below Sample 108-661A-10H-4, 45 cm; this sample contains *Discoaster hamatus*, abundant middle/late Miocene discoasters, and *Catinaster calyculus* without *Catinaster colatus*. Thus, this sample represents Zone CN7b and has an estimated age of 8.9–9.0 Ma. About 50 samples were examined between Samples 108-661A-10H-4, 140 cm, and 108-661A-12H-6, 103 cm, but all were barren of calcareous nannofossils. Thus, 22 m of sediment representing a time interval of about 57–58 m.y. separate the upper Miocene from the Upper Cretaceous.

#### Mesozoic (Maestrichtian-Campanian)

Upper Cretaceous sediments recovered from Site 661 are Maestrichtian and uppermost Campanian in age. They contain severely dissolved nannofossils (Table 7). Calcite overgrowth is especially common on specimens of the dissolution-resistant genus *Micula* and *Quadrum* spp. At this site the Late Cretaceous abundance fluctuations of nannofossils seems to be caused most likely by differential diagenesis rather than by ecological influences. The first sediment bearing Upper Cretaceous nannofossils is found in Sample 108-661A-12H-6, 121 cm, and contains few, moderately well-preserved species such as *Micula staurophora*, *Micula murus*, and *Micula prinsii*.

These corrosion-resistant species, accompanied by *Arkhangelskiella cymbiformis*, *Cribrospharella danae*, *Prediscosphaera grandis*, *Zygodiscus spiralis*, and *Microhabdulus stradneri*, constitute an assemblage characteristic of the upper portion of the *M. murus* Zone. *Micula prinsii*, the zonal marker for the top of the Maestrichtian, was observed from Samples 108-661A-13H-1, 100 cm, to Sample 108-661A-12H-6, 121 cm. The FO of *M. murus* observed in Sample 108-661A-13H-6, 100 cm, marks the base of the *M. murus* Zone.

At Site 661A, *Nephrolithus frequens*, an upper Maestrichtian marker fossil from higher latitudes, was not found, as it was in the South Atlantic. Therefore, I consider the absence of *N. frequens* to be a consequence of ecological exclusion rather than an indication of a hiatus below the *M. murus* Zone. Stratigraphically below the FO of *M. murus*, the preservation of the assemblage deteriorated, and only rare, poorly preserved fragments of *L. quadratus* were observed.

The LO of *Quadrum trifidum* occurs in Sample 108-661A-14H-8, 84 cm, but the FO of *Q. trifidum* was not reached in Hole 661A. The LO of *Reinhardtites levis* in Sample 108-661A-14H-7, 140 cm, seems a good indicator of the lower part of the *A. cymbiformis* Zone (in the absence of *L. quadratus*). The LOs of *Eiffelithus eximus* and *Reinhardtites anthophorus* were observed in Sample 108-661A-18X-2, 100 cm, according to different authors. The top of the range of these two coccoliths marks the upper Campanian boundary.

#### Site 662

Two holes were cored at Site 662, located in water depths of 3804 m, in order to investigate the history of the divergence in the equatorial Atlantic. The oldest sediments cored are early Pliocene in age. Calcareous nannofossils are abundant at Site 662. Most assemblages are moderately well preserved, with occasional poor preservation due to dissolution. Reworked discoasters in the Pleistocene were observed in the majority of samples investigated. Generally, this reworking is attributable to the presence of slumps and turbidites. Therefore, Pliocene and Pleistocene nannofossil assemblages are commonly severely intermixed between Sections 108-662A-10H-6 and 108-662A-12H-2.

The Pliocene/Pleistocene nannofossil assemblages at Site 662 are very similar in composition to those observed in previous Leg 108 sites, with the exception that *Umbilicosphaera mirabilis* composes a greater share of the total assemblage at Site 661.

At Site 662, located in an equatorial area, I was surprised to find that discoasters were minor components of the total assemblage (5%–10%).

#### Pleistocene

*Coccolithus pelagicus* was never observed in upper or middle Pleistocene assemblages; however, this species was a consistent, if rare, component of upper Pliocene and lowest Pleistocene assemblages. *Helicosphaera sellii* was present in sediment immediately below the slump that begins in Section 108-662A-12H-2. All major slumps occur from Section 108-662A-12H-2 and upward shortly above the extinction of *Calcidiscus macintyrei* in Sample 108-662A-13H-1, 75 cm, and downward.

Because late Pliocene nannofossil biostratigraphy is entirely based on discoaster events, their low abundance and reworking at Site 662 suggest the necessity of more detailed quantitative analysis. *Discoaster brouweri* and *Discoaster triradiatus* disappear between Samples 108-662A-14H-4, 150 cm, and 108-662A-14H-5, 75 cm (Table 8). Below these samples the very rare specimens of *D. brouweri* were considered reworked. In Hole 662B these events occur in Core 108-662B-6H, but they are difficult to determine due to intense reworking.

*Discoaster pentaradiatus* has its LO in Sample 108-662A-17H-2, 142 cm, and *Discoaster surculus* in Sample 108-662A-17H-3, 118 cm. Their occurrences at shallower levels most likely result from reworking. I was unable to determine the actual LOs of *Discoaster pentaradiatus*, *D. surculus*, and *D. tamalis* in Hole 662B because of the coarse sampling interval and the relative low abundance of discoasters. The extinction of *Reticulofenestra pseudoumbilica* between Samples 108-662A-22H-3, 50 cm, and 108-662A-22H-1, 70 cm, means that the latest part of the early Pliocene is represented.

#### Site 663

Two holes were drilled at Site 663, a companion site to Site 662, in water depths of 3698 m. The sediments recovered are

Table 7. Distribution of Pleistocene to late Campanian calcareous nannofossils, Hole 661A.

Age	Zonation Okada and Bukry, 1980	Zonation Martini, 1971	Preservation	Abundance	Core, section, interval (cm)	Sphenolithus abies/meadows												
						Pliocene			Miocene			middle			late			Pleistocene
						R	F	R	R	F	R	R	C	C	C	R	R	R
CN14a		NN20	G	A	1H-CC													
			G	A	2H-3, 80-81													
			G	C	2H-5, 80-81													
CN13b		NN19	M	A	3H-CC													
			M	A	4H-5, 80-81													
CN13a		NN19	M	A	4H-6, 80-81													
			M	A	4H-7, 40-41													
			M	A	5H-4, 80-81													
CN12d		NN18	M	A	5H-6, 80-81													
			M	A	6H-2, 80-81													
			M	A	7H-4, 24-25													
CN12c		NN17	P	C	4H-6, 80-81													
			M	A	4H-7, 40-41													
			M	A	5H-4, 80-81													
CN12a-b		NN16	M	A	5H-6, 80-81													
			M	A	6H-2, 80-81													
			M	A	7H-4, 24-25													
CN11/10		NN15/14	M	A	7H-4, 90-91													
			M	A	7H-6, 90-91													
			M	A	8H-6, 90-91													
CN10b		NN13	M	A	8H-6, 150-151													
			M	A	9H-1, 10-11													
			M	A	9H-1, 90-91													
CN10a		NN12	M	A	9H-4, 50-51													
			M	A	9H-CC													
			M	A	10H-1, 70-71													
CN9		NN11	M	A	10H-1, 110-111													
			M	A	10H-3, 130-131													
			M	A	10H-3, 150-151													
CN8		NN10	M	A	10H-4, 45-46													
			M	A	10H-3, 150-151													
			M	A	10H-4, 45-46													
CN7		NN9	M	A	10H-3, 150-151													
			M	A	10H-4, 45-46													

Age	Zones	Preservation	Abundance	Core, section, interval (cm)	Ceratolithoides aculeatus												
					Rhagodiscus angustus			Reinhardtites anthophorus			Wattnaueria barnesae			Lithraphidites carniolensis			Biscutum constans
					R	F	R	R	R	F	C	C	F	R	R	R	R
Maestrichtian	Micula murus	P	A	12H-6, 121-125													
				12H-6, 122-125													
				12H-6, 124													
				12H-1, 30-31													
				13H-1, 60-61													
				13H-1, 100-101													
				13H-1, 145-146													
				13H-2, 140-141													
				13H-4, 105-106													
				13H-5, 72-73													
early	Arkhan. cymb.	M	A	13H-6, 100-101													
				14H-5, 80-81													
				14H-7, 140-141													
				14H-8, 84-85													
				15H-3, 100-101													
				15H-4, 140-141													
				15H-CC													
				16X-CC													
				17X-CC													
				18X-1, 105-106													
late	Quadrat. trifidum	M	A	18X-2, 100-101													
				18X-CC													



**Table 8.** Distribution of Pleistocene to early Pliocene calcareous nannofossils, Hole 662A.

late Pliocene through Holocene in age. The pelagic sedimentation at Site 663 is interrupted by several major slumps or turbidites (<45 m in total thickness), creating massive reworking at some levels and inverted stratigraphic orders of biostratigraphic datums within other intervals. About two-thirds of the Pleistocene appears undisturbed, although reworking of Pliocene sediment was evident at many levels. In contrast some intraslump units seem unaffected by sediment mixing.

The composition, preservation, and abundance of nannofossil assemblages are very similar to that of Site 662 (e.g., generally low discoaster abundance, absence of *Coccolithus pelagicus* in most of the Pleistocene sequence, and high abundances of helicosphaerids, rhabdosphaerids, and syracosphaerids).

## *Pleistocene*

Table 9 gives the range chart of species examined in Hole 663A.

## *Pliocene*

*Discoaster brouweri* and *D. triradiatus* were examined in low, but consistent numbers (>1 specimen/5 fields of view at a particle density of about 200/field of view) from Sample

108-663A-12H-3, 100 cm, and downward. A major reduction in the abundance of *Discoaster asymmetricus* was observed in conjunction with the LO of *Discoaster tamalis* between Samples 108-663A-16H-3, 90 cm, and 108-663A-16H-4, 100 cm.

## Site 664

Site 664 is located in a water depth of 3806.5 m in the central equatorial Atlantic on the upper middle flank on the east side of the mid-Atlantic Ridge just north of the Romanche Fracture Zone. Four holes were drilled, but Hole 664A was abandoned after one core. All other holes were continuously cored. The presence of extensive slumps and turbidites in Hole 664B results in considerable stratigraphic complexity, although in Hole 664D the normal stratigraphic sequence was only slightly altered.

Discoasters are substantially more abundant at Site 664 than at Sites 662 and 663. Placoliths are moderately dissolved in the latest Miocene through Pleistocene and are severely dissolved in the earliest late Miocene. Discoasters show moderate overgrowth throughout the latest Miocene and Pliocene. Overgrowth increases in the late Miocene, and most primary morphological characters in the earliest last Miocene are severely blurred by secondary calcite.

**Table 9. Distribution of Pleistocene to late Pliocene calcareous nannofossils, Hole 663A.**

Hole 664B

### *Pleistocene*

The first major slump was found in Core 108-664B-6H, and samples investigated above the slump in Core 108-664B-6H all lacked *Helicosphaera sellii* and *Calcidiscus macintyrei*.

### *Pliocene*

Sample 108-664B-6H-4, 30 cm, taken from the uppermost part of the slump, and Core 108-664B-8H contained an upper Pliocene assemblage, including *Discoaster asymmetricus* and *Discoaster tamalis*, whereas Cores 108-664B-9H and -10H show a reworked assemblage that suggests an early Pliocene age, with common *Reticulofenestra pseudoumbilica* and sphenoliths.

In the sediments of Cores 108-664B-11H and -12H that were disturbed by slumping, no reworking was observed; the discoaster assemblage represents a late Pliocene age, with common *Discoaster brouweri* and very rare *Discoaster pentaradiatus*. Cores 108-664B-13H through -19H contain upper Pliocene discoasters, including *D. tamalis*. In this interval, several cores affected by turbidites, debris flows, or slumps yielded rare lower Pliocene nannofossils.

Although Cores 108-664B-20H and -21H contain slumped units, they seem biostratigraphically undisturbed, suggesting the LO of sphenoliths in Core 108-664B-20H and that of *R. pseudoumbilica* in Core 108-664B-21H.

**Hole 664D**

### *Pleistocene*

Cores 108-664D-1H and -2H show typical upper Pleistocene assemblages, characterized by low species diversity and a strong dominance of gephyrocapsids (Table 10).

### *Pliocene*

The succession of upper Pliocene assemblages is broken in Core 108-664D-13H by a slump representing sediment of early Pliocene age. The Miocene discoasters show substantial overgrowth of the central area and placoliths show strong etching, making difficult their distinction and a precise stratigraphic attribution.

In the early part of the late Miocene, the dissolution has strongly altered the composition of the nannofossil assemblages constituted of abundant discoasters and few plankoliths.

### Site 665

Site 665 is located in the eastern equatorial Atlantic along the base of the southeastern margin of the Sierra Leone Rise, at 4741 m water depth. The two holes drilled at this site contained a continuous normal biostratigraphic record of the Holocene through lower Pliocene. There was little evidence of the slumps and turbidites that characterized previous holes (i.e., Sites 662, 663, and 664).

Below Sample 108-665A-9H-5, 135 cm, sediments are barren of nannofossils. Nannofossil preservation at Site 665 is good only in the first two cores (Holocene), moderate in the lower Pleistocene, and poor in the Pliocene. I observed severe etching and dissolution of the placoliths and overgrowth on the discoasters in the Pliocene assemblages, although many lower Pliocene samples show beautifully preserved discoaster assemblages.

Pleistocene

As at Site 664, species diversity is low.

**Table 10.** Distribution of Pleistocene to late Miocene calcareous nannofossils, Hole 664D.

**Table 11.** Distribution of Pleistocene to early Pliocene calcareous nannofossils, Hole 665A.

Age	Zonation Okada and Bukry, 1980		Zonation Martini, 1971		Preservation	Abundance	Core, section, interval (cm)	Sphenolithus abies/hecabies Ceratolithus acutus Amaurolithus amplificatus Oolithus antillarum Scyphosphaera aposteini Discosaster asymmetricus Discosaster brouweri Gephyrocapsa caribbeonica Rhabdosphaera clavigera Ceratolithus cristatus Amaurolithus delicatus Crenolithus doronicoides Discolithina japonica Helicosphaera kampnieri Pseudomediania lacunosa Calcidiscus leptoporus Calcidiscus macintyreii Umbilicosphaera mirabilis Discosaster neohamatus Gephyrocapsa oceanica Coccolithus pelagicus Discosaster pentadrianus Amaurolithus primus Reticulofenestra pseudounbilicala Scyphosphaera pulcherrima Syracosphaera pulchra Discosaster quinqueramus Ceratolithus rugosus Helicosphaera sellii Umbilicosphaera sibogae Reticulofenestra "small" Gephyrocapsa spp. Rhabdosphaera stylifer Discosaster surculus Pontosphaera syracusana Discosaster tamalis Amaurolithus tricorniculatus Discosaster triradiatus Discosaster variabilis	
	Pleistocene	late	early	Pliocene					
CN14b	NN20	G	A	1H-CC					
		G	A	2H-3, 134–135					
		G	A	2H-5, 60–61					
		M	A	3H-CC					
		M	A	4H-3, 150–151					
		M	A	4H-4, 10–11					
		M	A	4H-6, 130–131					
		M	A	5H-3, 120–121					
CN14a	NN19	F	F						
		F	F						
		R	R						
		R	F						
		R	F						
		R	F						
		R	F						
		R	F						
CN13b	NN19	A	R						
		A	R						
		A	F						
		A	R						
		A	R						
		C	R						
		C	R						
		R	F						
CN13a	NN19	A	R						
		A	R						
		A	R						
		A	R						
		A	R						
		A	R						
		R	F						
		R	F						
CN12d	NN18	M	A	5H-4, 30–31					
		P	A	5H-6, 30–31					
		P	A	5H-6, 90–91					
		P	A	5H-6, 90–91					
		P	A	6H-4, 80–81					
		P	A	6H-5, 90–91					
		P	A	6H-7, 10–11					
		M	A	7H-1, 80–81					
CN12c	NN17	M	A	7H-CC					
		M	A	8H-3, 90–91					
		R	F						
		R	F						
		C	C						
		C	C						
		R	F						
		R	F						
CN12b	NN16	R	F						
		F	C						
		F	C						
		C	C						
		C	C						
		R	F						
		R	F						
		R	F						
CN12a	NN16	M	A	8H-3, 90–91					
		R	F						
		F	C						
		F	C						
		C	C						
		C	C						
		R	F						
		R	F						
CN11	NN15/13	P	A	8H-4, 100–101	C				
		P	A	8H-CC	A				
		P	A	9H-1, 50–51	A				
		P	A	9H-3, 77–78	A				
		P	A	9H-3, 140–141	A				
		P	M	9H-4, 30–31	C				
		P	M	9H-5, 25–26	R				
		P	M	9H-5, 32–33	C				
CN10c	NN15/13	P	M	9H-5, 135–136	C				
		P	M	9H-5, 135–136	R				
		F	C						
		F	C						
		R	F						
		R	F						
		C	C						
		C	C						
CN10b	NN12	P	A	8H-4, 100–101	C				
		P	A	8H-CC	A				
		P	A	9H-1, 50–51	A				
		P	A	9H-3, 77–78	A				
		P	M	9H-3, 140–141	C				
		P	M	9H-4, 30–31	R				
		P	M	9H-5, 25–26	C				
		P	M	9H-5, 32–33	R				
CN10a	NN12	P	M	9H-5, 135–136	C				
		P	M	9H-5, 135–136	R				
		F	C						
		F	C						
		R	F						
		R	F						
		C	C						
		C	C						

**Table 12. Distribution of Pleistocene to early Pliocene calcareous nannofossils, Hole 666A.**

Table 13. Distribution of Pleistocene to early Pliocene calcareous nannofossils, Hole 667A.

Age	Zonation Okada and Bukry, 1980	Zonation Martin, 1971	Preservation	Abundance	Core, section, interval (cm)	<i>Sphenolithus abies/neobabies</i>	<i>Cyclargolithus abisectus</i>	<i>Ceratolithus acutus</i>	<i>Discoaster adamantis</i>	<i>Helicosphaera ampliaperta</i>	<i>Amaurolithus amplificus</i>	<i>Oolithus antillarum</i>	<i>Discoaster asymmetricus</i>	<i>Sphenolithus belemnos</i>	<i>Discoaster bellus</i>	<i>Discoaster berggrenii</i>	<i>Zygrhabolithus bijugatus</i>	<i>Discoaster brouweri</i>	<i>Catinaster calyculus</i>	<i>Gephyrocapsa caribbeanica</i>	<i>Triquetorhabdus carinatus</i>	<i>Discoaster challengerii</i>	<i>Sphenolithus cipriensis</i>	<i>Rhabdosphaera clavigera</i>	<i>Catinaster coalitus</i>	<i>Helicosphaera compacta</i>	<i>Sphenolithus conicus</i>	<i>Ceratolithus cristatus</i>	<i>Reticulofenestra daviesi</i>	<i>Discoaster deflandrei</i>
Pleistocene	CN14b	NN20	G G G	C A A	1H-CC 2H-3, 110-111 2H-4, 110-111 2H-4, 120-121 3H-CC 4H-CC										r															
	CN14a	NN19	M M M	A A A																										
	CN13		M M	A A																										
Pliocene	CN12d-c	NN18	M M	A A	5H-2, 90-91 5H-3, 110-111 5H-5, 114-115 6H-2, 80-81				R																					
	CN12a-b	NN17	M M	A A	6H-CC 7H-1, 50-51 7H-1, 135-136	F C			R F R R																					
	CN11	NN16	M M	A A	7H-CC 8H-CC	A C			R R																					
	CN10d	NN15/14	M M	A A	9H-6, 52-53	C C																								
	CN10c	NN13	M M	A A	10H-1, 101-102	C C			R																					
	CN10a-b	NN12	M M	A A	10H-5, 86-87	C C			R																					
Miocene	Late middle	CN9	M M	A A	10H-6, 31-32 11H-CC 12H-CC 13H-2, 100-101	C C C																								
		NN11	M M	A A	13H-CC 14H-3, 120-121 14H-CC	C C C																								
		CN8	M M	A A	14H-CC	F																								
	early	CN4	M P	A A	15H-CC 16H-CC 17H-4, 100-101	F F F																								
		NN5	P P	A A	17H-CC 17H-4, 100-101	F F F																								
		NN7	P P	A A	18H-1, 70-71	R R R																								
Oligocene	NN6	NN6	P P	A A	18H-5, 110-111	R R																								
		NN5	P P	A A	19H-5, 100-101	A F			R R																					
		CN4	M M	A A	20H-CC 21H-CC 22H-CC	R R																								
	CN1a	NN4	P M	A A	23H-CC 24X-CC	R																								
		NN3	P P	A A	25X-CC	C R																								
		CN1c	P P	C A	26X-CC 27X-CC	C F																								
Oligocene	CN1b	NN2	P P	A A	28X-CC 29X-CC	C F																								
		NN2/ NN1	P P	A A	30X-CC	C C																								
		NN1	P P	C A	31X-CC	C C																								
	CN1a	NN1/ NP25	P P	A A	32X-5, 90-91	C C																								
		NP25	M M	A A	33X-CC	C C																								
		NP25	M M	A A	34X-CC	F R																								
Oligocene	CP19b	NP25	M P	A A	35X-CC 36X-CC	C C																								
	CP19a	NP24	M M	A A	37X-5, 127-128 38X-CC 39X-CC	F																								
	CP18	NP24/23	M M	A A	40X-2 40X-CC 41X-3 41X-CC																									

Table 13. (continued).

Age	Zonation Okada and Bukry, 1980	Zonation Martini, 1971	Preservation	Abundance	Core, section, interval (cm)	<i>Amurolithus primus</i>	<i>Reticulofenestra pseudoumbilica</i>	<i>Syphosphaera pulcherrima</i>	<i>Syracosphaera pulchra</i>	<i>Discaster quinqueramus</i>	<i>Helicosphaera recta</i>	<i>Cyclolithella rotula</i>	<i>Ceratolithus rugosus</i>	<i>Triquetrorhabdulus rugosus</i>	<i>Helicosphaera sellii</i>	<i>Orthorhabdulus serratus</i>	<i>Umbilicosphaera sibogae</i>	<i>Reticulofenestra "small"</i>	<i>Gephyrocapsa</i> spp.	<i>Rhabdosphaera stylifer</i>	<i>Discaster surculus</i>	<i>Discaster tamalis</i>	<i>Ceratolithus tricorniculatus</i>	<i>Discaster irridiatius</i>	<i>Helicosphaera truemppii</i>	<i>Discaster variabilis</i>
Pleistocene	CN14b	NN20	G	C	1H-CC																					
	CN14a		G	A	2H-3, 110-111																					
	CN13		G	A	2H-4, 110-111																					r
Pliocene	CN12d-c	NN18	M	A	5H-2, 90-91																					
	CN12d-c		M	A	5H-3, 110-111																					
	CN12a-b	NN17	M	A	5H-5, 114-115																					
	CN12a-b		M	A	6H-2, 80-81																					
	CN11	NN16	M	A	6H-CC																					
	CN11		M	A	7H-1, 50-51																					
	CN10d	NN15/14	M	A	7H-1, 135-136																					
	CN10c		M	A	7H-CC																					
Miocene	CN10a-b	NN13	M	A	8H-CC																					
	CN10a-b		M	A	9H-6, 52-53																					
	CN10d	NN12	M	A	10H-1, 101-102																					
	CN10c		M	A	10H-5, 86-87																					
	CN9	NN11	M	A	10H-6, 31-32																					
	CN9		M	A	11H-CC																					
	CN8	NN10	M	A	12H-CC																					
	CN8		M	A	13H-2, 100-101																					
Miocene	CN4	NN5	M	A	13H-CC																					
	CN4		P	A	14H-3, 120-121																					
	CN5	NN7	M	A	14H-3, 120-121																					
	CN5		P	A	14H-CC																					
	CN4	NN6	M	A	15H-CC																					
	CN4		P	A	16H-CC																					
	CN1c	NN2	M	A	17H-4, 100-101																					
	CN1b	NN2/ NN1	P	A	17H-CC																					
	CN1a	NN1	M	A	18H-1, 70-71																					
	CN1a		P	A	18H-5, 110-111																					
Oligocene	CN3	NN4	M	A	19H-5, 100-101																					
	CN2		M	A	20H-CC																					
	CN1c	NN2	P	A	21H-CC																					
Oligocene	CN1b	NN2/ NN1	M	A	22H-CC																					
	CN1a		P	A	23H-CC																					
	CN1a	NN1/	M	A	24X-CC																					
Oligocene	CP19b	NP25	P	A	25X-CC																					
	CP19a		M	A	26X-CC																					
	CP18	NP24/23	P	A	27X-CC																					
Oligocene	CP19b	NP25	M	A	28X-CC																					
	CP19a	NP24	P	A	29X-CC																					
	CP18	NP24/23	M	A	30X-CC																					
Oligocene	CP19b	NP25	M	A	31X-CC																					
	CP19a	NP24	M	A	32X-5, 90-91																					
	CP18	NP24/23	M	A	33X-CC																					
Oligocene	CP19b	NP25	M	A	34X-CC																					
	CP19a	NP24	M	A	35X-CC																					
	CP18	NP24/23	M	A	36X-CC																					

**Table 13.** (continued).

Table 14. Distribution of Pleistocene to late Pliocene calcareous nannofossils, Hole 668A.

Age	Zonation Okada and Bukry, 1980	Zonation Martini, 1971	Preservation	Abundance	Core, section, interval (cm)	<i>Discoaster brouweri</i>										<i>Gephyrocapsa caribbeanica</i>										<i>Rhabdosphaera clavigera</i>										<i>Crenolithus doronicoides</i>										<i>Syracosphaera histrica</i>																																											
						<i>Discoaster brouweri</i>					<i>Gephyrocapsa caribbeanica</i>					<i>Rhabdosphaera clavigera</i>					<i>Crenolithus doronicoides</i>					<i>Syracosphaera histrica</i>					<i>Pontosphaera japonica</i>					<i>Helicosphaera kampneri</i>					<i>Pseudodemania lacunosa</i>					<i>Calcidiscus mucintyrei</i>					<i>Umbilicosphaera mirabilis</i>					<i>Gephyrocapsa oceanica</i>					<i>Coccolithus pelagicus</i>					<i>Scyphosphaera sp.</i>					<i>Helicosphaera sellii</i>					<i>Reticulofenestra "small"</i>					<i>Gephyrocapsa spp.</i>					<i>Ceratolithus rugosus</i>			
Pleistocene	CN14b	NN20	G	A	1H-CC	A	C	C	F	C	R	A	R	F	C	R	C	R	C	R	F	C	F	A	C	F	A	C	R	F	A	R	F	F	A	F	F	A	R	F	F	A	F																																														
			G	A	2H-4, 130	A	C	C	F	C	R	C	R	F	C	R	C	R	C	R	F	C	F	A	C	F	F	F	F	R	F	R	R	F	F	F	R	F	F	R	F																																																
			G	A	2H-6, 130	A	F	C	F	R	C	R	C	F	C	R	C	R	C	R	F	C	F	A	C	F	F	F	R	F	R	R	F	F	F	R	F	F	R	F																																																	
			G	A	2H-CC	A	F	C	F	R	C	R	C	F	C	R	C	R	C	R	F	C	F	A	C	F	F	F	R	F	R	R	F	F	F	R	F	F	R	F																																																	
late Pliocene	CN13b	NN19	G	A	3H-3, 97-98	A	F	C	F	R	C	R	C	F	C	R	C	R	C	R	F	C	F	A	C	F	F	F	R	F	R	R	F	F	F	R	F	F	R	F																																																	
			G	A	3H-5, 130-131	A	C	C	F	R	C	R	C	F	C	R	C	R	C	R	F	C	F	A	C	F	F	F	R	F	R	R	F	F	F	R	F	F	R	F																																																	
			G	A	3H-CC	C	C	C	F	R	C	R	C	F	C	R	C	R	C	R	F	C	F	A	C	F	F	F	R	F	R	R	F	F	F	R	F	F	R	F																																																	
			M	A	4H-1, 110-111	C	C	C	F	R	C	R	C	F	C	R	C	R	C	R	F	C	F	A	C	F	F	F	R	F	R	R	F	F	F	R	F	F	R	F																																																	
	CN13a		M	A	4H-2, 130-131	F	C	C	F	R	C	R	C	F	C	R	C	R	C	R	F	C	F	F	F	F	R	F	R	R	F	F	F	R	F	F	R	F																																																			
			M	A	4H-5, 110-111	C	C	F	R	A	F	F	F	F	R	A	F	F	F	R	F	C	F	F	F	F	R	F	R	R	F	F	F	R	F	F	R	F																																																			
			NN18	M	4H-6, 40-41	R	F	C	C	F	C	F	F	F	R	C	F	F	C	F	F	C	F	F	F	F	R	F	F	F	A	R	R	F	F	F	R	F	F	R																																																	
	CN12d		M	A	4H-6, 140-141	F	F	C	C	F	C	F	F	F	R	C	F	F	C	F	F	C	F	F	F	F	R	F	F	F	A	R	F	F	F	R	F	F	R																																																		
			M	A	4H-CC	F	C	C	C	R	C	F	F	F	R	C	F	F	C	F	F	C	F	F	F	R	F	F	F	A	R	F	F	F	R	F	F	R																																																			

**Pliocene**

A normal succession of Pliocene discoasters allowed good biostratigraphic control (Table 11).

**Site 666**

Site 666 makes up part of a depth transect across the southern flank of the Sierra Leone Rise and was drilled in 4517 m water depth. The site consists of a single hole that extends down to the lower Pliocene. Every core of Site 666 contains intervals in which the nannofossil assemblages represent mixtures of different biostratigraphic zones (Table 12). Approximately 50% of the Pliocene and Pleistocene sediments reflect pelagic deposition, the other half being composed of turbidites varying in thickness from a few centimeters to about 12 m.

To obtain an elementary biostratigraphic understanding of the sequence, I have attempted to exclude samples taken from turbidites, samples that contain obvious reworking, and samples that show no reworking but in which assemblages of an older age overlie stratigraphically younger ones. The reworking is generally restricted to late Neogene species. Preservation is moderate in terms of placolith dissolution and discoaster overgrowth. In the red-clay facies (Core 108-661A-16H), dissolution is intense and has also affected the discoasters, entailing great abundances of isolated rays or fragments of rays.

**Pliocene**

Sediments investigated from Core 108-666A-12H showed intervals in which the Pliocene discoasters were mixed with obviously reworked forms of Pliocene/early Pleistocene assemblages. Yet, samples from Core 108-666A-13H display assemblages characteristic of the early part of the late Pliocene, containing *Discoaster tamalis* and *D. asymmetricus* but lacking sphenoliths and *Reticulofenestra pseudoumbilica*. Well-preserved specimens of *Ceratolithus rugosus* and *C. acutus* were recognized from the red clay facies in Core 108-666A-16H, which affirmed that Hole 666A terminated in basal Pliocene sediment.

**Site 667**

Site 667 was the third site on the south slope of the Sierra Leone Rise and was located in 3535 m water depths. Two holes were drilled, and the 41 cores retrieved from Hole 667A yielded Oligocene through Pleistocene nannofossil assemblages, the majority of which show moderate preservation.

**Pleistocene**

Glacial and interglacial cycles are represented by alternating dark and white oozes. Small gephyrocapsids were present in great abundance as "blooms" in Sample 108-667A-3H-4, 120 cm, possibly indicating the "small Gephyrocapsa acme Zone." In some Pleistocene samples *Helicosphaera carteri* and *Umbilicosphaera mirabilis* were abundant. Samples 108-667A-3H-CC and 108-667A-4H-CC contained common Pliocene discoasters and placoliths, as well as some early Miocene placoliths and discoasters, indicating that these assemblages reflect partial reworking.

**Pliocene**

Pliocene discoasters occurred in great abundances but showed reworking at Site 667, making their extinction level uncertain (Table 13).

**Miocene**

Reticulofenestrads are the dominant assemblage component in the upper Miocene sediments. In several of the upper Miocene samples, the amaurolithid/total assemblage ratio (<1:10,000) suggested that the FO of amaurolithids can easily be missed.

Core 108-667A-15H to Section 108-667A-17H-5 correspond to obvious slump deposits in which nannofossil assemblages are composed of mixtures of early middle and early Miocene taxa.

The different Miocene zonal markers were recognized at Site 667 without reworking and allow good biostratigraphic control. In the lower Miocene assemblages, placoliths presented good to moderate preservation, whereas the discoasters (in particular, *Discoaster deflandrei*) were overgrown.

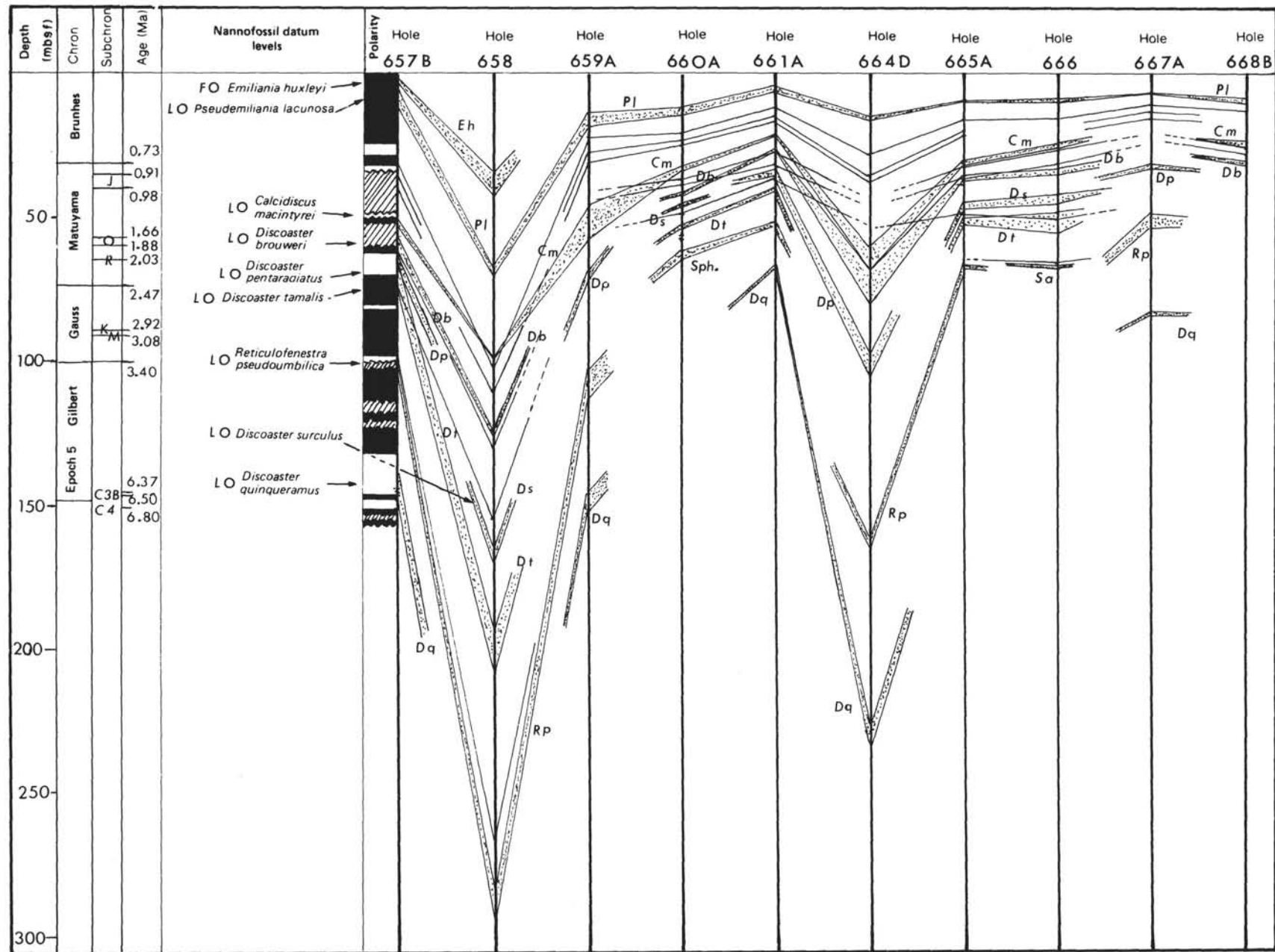


Figure 3. Correlation of selected calcareous nannofossil events to the paleomagnetic results (Tauxe et al., this vol.) plotted vs. depth for Leg 108 holes.

Although many samples were investigated from Cores 108-667A-28X to -35X, I did not recognize consistent occurrences of Oligocene species in that interval, except for one specimen of *Helicosphaera recta* in Sample 108-667A-32X-5, 90 cm, and Section 108-667A-35X-CC, as well as rare specimens of *Dictyococcites bisectus* in Core 108-667A-33X.

#### Oligocene

The almost absence of *Discoaster bisectus* and *Helicosphaera recta* made the Oligocene/Miocene boundary approximate by the LO of *Sphenolithus ciperoensis*. Unfortunately, the Oligocene sphenolith marker species *S. ciperoensis*, *S. distensus*, and *S. predistensus* occur only sporadically. Counts of *S. ciperoensis* from the core-catcher samples of Cores 108-667A-33X through -38X, result in no *S. ciperoensis* in Core 108-667A-33X, one specimen in Core 108-667A-34X, two specimens in Core 108-667A-35X, and >10 specimens in Cores 108-667A-36X through -38X. Thus, I have placed the Oligocene/Miocene boundary tentatively within Core 108-667A-36X, based on the marked decrease in abundance of *S. ciperoensis*. The boundary, however, may occur as high as Core 108-667A-32X, where a single specimen of *H. recta* was found.

#### Site 668

Site 668 was the last site in the Sierra Leone Rise transect. Only four cores were taken in Hole 668B, indicating a tropical environment and little evidence of reworking in any of the samples studied. The latest Pliocene through Pleistocene nannofossil assemblages at Site 668 show good preservation and contain three reliable species events (Table 14). Hole 668A is represented by a single core, of which the core-catcher sample represents a level above the extinction of *Pseudoemiliania lacunosa*.

#### DISCUSSION

Despite the sedimentation disturbances due to slump and turbidites in several sites, creating massive reworking at some levels, a comprehensive study of the coccolith abundance, preservation assemblages, and biostratigraphic sequences reveals through time some characteristic paleoenvironmental trends for Leg 108.

#### Preservation, Abundance, and Diversity

At Leg 108 sites, the preservational variability of nannofossils reflects the diverse lithologies, the degrees of diagenesis of the sediments, and the differences in surface productivity. Intervals of poorly preserved nannofossils are located in the Miocene clays (Sites 659–667), in the Pliocene of the deep-water sites (Sites 657, 660, 665, and 666), or at sites located under waters of high surface productivity (Sites 660–665).

In these depositional environments, an intense dissolution fragmented the placoliths, etched many small species, and produced an overgrowth of discoasters. These diagenetic transformations are often linked to dissolution of carbonates induced by a water depth below the calcite-compensation depth (CCD) or by upwelling with a high input of terrigenous material.

Nannofossil abundance and preservation are also influenced by bottom currents and especially by the Canary and Benguela cold currents (Sites 658, 659, and 662–664).

In the Pleistocene, the nannofossil assemblages present virtually identical abundances, species diversity, and preservation at all sites. The best preservation is observed within the late Pleistocene Zones NN21 and NN20. These assemblages are dominated by *Gephyrocapsa caribbeanica*, *G. oceanica*,

and other small *Gephyrocapsa* spp. not separated in this chapter. The interval of dominant small *Gephyrocapsa* recognized in the middle Pleistocene of several sites probably represents the “small *Gephyrocapsa* acme Zone” of Gartner (1977), correlatable to the Jaramillo Subchron, and probably indicates a time of increased productivity, apparently widespread and in connection with a major change in ocean circulation (Gartner et al., 1987).

Common elements characteristic of warm water include *Calcidiscus leptoporus* var. B, known to be the most solution-resistant species, and *Helicosphaera carteri*, which can be abundant in Pliocene Zones NN17–NN16 and then decreases in the Pleistocene. This last tropical-subtropical species was recognized in great abundance with *Umbilicosphaera sibogae* and *U. mirabilis* in equatorial Sites 662–663.

The common occurrence of rhabdosphaerids, scyphosphaerids, and syracosphaerids indicates subtropical conditions during the Pliocene (Sites 666–667), whereas the low abundance of rhabdosphaerids and discoasters was accompanied by a high abundance of *Reticulofenestra* spp. and *Coccolithus pelagicus*. These fluctuations are characteristic of cooler water species in the upwelling environment of Site 658.

In the late Pliocene, *C. pelagicus* only occurred in cold as well as tropical sites. The maximum of frequency was observed in Zones NN17–NN18; then this taxon disappeared from the community at the beginning of the Pleistocene (Sites 666–667). The size of *Gephyrocapsa* sp. in the late Pliocene seems to increase toward the top of Zone NN18.

A second group of common Pliocene coccoliths is constituted of *Pseudoemiliania lacunosa*, *Crenalithus doronicoides*, and *Calcidiscus macintyreai*. The latter taxon is generally common to abundant at all the sites, but the abundance of *C. doronicoides* decreases in the lower part of the Pleistocene and the late Pliocene. The oscillations of abundances of this species show a slight positive correlation with that of *C. macintyreai* and *P. lacunosa*.

Usually in Leg 108, nannofossil species diversity is lower in the Pleistocene than in the Pliocene, where the discoasters, which are warm-water species and resistant to diagenesis, can be diverse in tropical and subtropical sites (660, 665, and 667). Yet, a low abundance of discoasters (>1% of the total assemblage) was observed at the intensely upwelling Site 658 due to postdepositional dissolution. At sites influenced by the Canary Current (659) or the Benguela Current (662–663), discoasters also are minor components of the assemblages. More detailed quantitative discoaster analyses might give an explanation for their low abundance.

The ceratoliths are few and generally poorly preserved with much secondary calcite. The evolutionary transition from *C. rugosus* to *Ceratolithus acutus* was tentatively recognized at Sites 657, 659, and 667.

In the upper Miocene sediments, the differences in nannofossil preservation are in connection with color cycles: the whitish cycles showing moderately dissolved placolith assemblages moderately to badly overgrown discoasters, whereas the reddish or bluish cycles are constituted of severely dissolved placoliths and well-preserved discoasters. The Miocene placoliths are broadly reduced to dissolution-resistant species. Placolith assemblages are dominated by reticulofenestrids in the middle and upper Miocene and by *Cyclicargolithus floridanus* in the lower Miocene.

At Site 659, under the Canary Current, blooms of *Reticulofenestra minuta* dominate all other taxa. After the “small” *Reticulofenestra* (Gartner et al., 1987), as well as the small *Gephyrocapsa* in the Pleistocene can be considered “opportunistic” species, broadly adapted to a range of environmental

conditions. Discoasters are diversified and abundant throughout the Miocene sediments. They are generally well preserved with the exception of overgrowth on *Discoaster quinqueramus* and *D. deflandrei*.

In the early Miocene, I noticed the presence of diverse helicosphaerids, such as *Helicosphaera euphratis*, *H. granulata*, *H. intermedia*, and *H. obliqua*, as well as the large *H. truempyi* in the very basal Miocene.

In the Oligocene (Site 667), the assemblages are generally similar to the lower Miocene ones in composition and abundance with a strong dominance of *Sphenolithus moriformis* and common *C. floridanus*. Yet in the low latitude of Site 667, the rare occurrence of other Oligocene sphenoliths and of helicosphaerids and the total absence of *Dictyococcites bisectus* were surprising.

### Biostratigraphic Remarks

No quantitative study was attempted of the different *Gephyrocapsa* species. The increase and FO of *Emiliana huxleyi* was investigated by SEM. Usually, Zone NN21 of uppermost Pleistocene was rather thin, as in open-ocean sediments and could often be missed. The other standard Pleistocene events were well recognizable though the appearances or extinctions were sometimes observed in low abundance and made imprecise the exact boundaries (*Pseudoemiliania lacunosa* and *Helicosphaera sellii* become very scarce toward their LO). On the other hand, the LO of *Calcidiscus macintyreai* generally more represented was used as a good zonal event.

At several sites, according to lower abundances, the LO of *Discoaster pentaradiatus* appears less reliable than the LO of *Discoaster surculus*. Therefore, placement of the top of Zone NN16 was considered more confident than that of the top of Zone NN17. Detailed investigation suggested that the LO of sphenoliths (*S. abies* and *S. neobabies*) were not synchronous with *Reticulofenestra umbilica*, as they could exist stratigraphically above the LO of *R. pseudoumbilica* (2–5 m at Sites 659, 660, and 661). This diachronism represented a time interval of 0.05–0.13 m.y. at Site 659.

Amaurolithids were never common and overgrown at Leg 108 sites and were even less numerous toward the end of their range; therefore, it was difficult to recognize the zonal boundary between NN15/NN14. On the other hand, if *Discoaster asymmetricus* was generally common between the LOs of *Reticulofenestra umbilica* and *Discoaster tamalis*, at the different sites, *D. asymmetricus* became rare below the LO of *R. pseudoumbilica* or even was not observed at some sites (665 and 666). Thus, this discoaster, contrary to some authors' opinions, was not a reliable marker for the base of Zone NN14, and at Leg 108 the zonal boundary NN14/NN13 cannot be recognized. The placement of the Zone NN12/NN13 boundary was also difficult to determine due to the rarity and overgrowth of *Ceratolithus rugosus* (Sites 658–659).

Usually, in Leg 108, because the amaurolithids and triquetrorhabdids were scarce and delicate forms (especially FO *C. acutus* and LO (*Triquetrorhabdulus rugosus*)), I have chosen the LO of *D. quinqueramus* as the best nannofossil to approximate the Miocene/Pliocene boundary. I noticed that *D. quinqueramus* continued its range at least 6 m above the LO of *Amaurolithus amplificus* at Site 657, thus indicating a diachronous extinction with that of *A. amplificus*, observed at other sites. Yet, the extinctions of these two species were suggested as synchronous by Berggren et al. (1985b).

*Triquetrorhabdulus carinatus*, the zonal marker of the top of the lowermost zone in the Miocene (CN1c), was rare toward its extinction (Section 108-667A-25X-CC), then it increased in abundance and finally, few to rare specimens continued down to Section 108-667A-36X-CC. A similar sharp

abundance decline followed by a long tail of rare occurrences was also recorded in the mid-latitude North Atlantic at DSDP Sites 558 and 563 by Parker et al. (1985).

At Site 667, the abundance of *Cyclargolithus abisectus* followed by a sharp abundance decline was not observed distinctly in any of the subsamples examined, as in Bukry's zonal concept (1973), who placed the Oligocene/Miocene boundary at the end of the acme interval of *C. abisectus*. Therefore, at Site 667, the Paleogene/Neogene boundary was determined by the LO of *Sphenolithus ciperoensis*, in the virtual absence of *Dictyococcites bisectus* and *Helicosphaera recta*. Yet in this late site, unfortunately the Oligocene sphenolith marker species only occur sporadically, making approximate the recognition of NP24 and NP23 Zones.

In the Upper Cretaceous sediments recognized in Hole 661A, the assemblages are constituted of dissolution-resistant species, which include, however, the principal zonal taxons *Micula prinsii*, *M. murus*, *Quadrum trifidum*, *Q. gothicum*, and species characteristic of the lower Maestrichtian/upper Campanian such as *Eiffelithus eximius*, *Reinhardtites anthophorus*, and *R. levis*. I noticed the absence of *Lucianorhabdus cayeuxi*, a typical nearshore indicator, and that of *Nephrolithus frequens*, a high-latitude taxon. These "absences," associated with the abundance of *Quadrum trifidum* and *Q. gothicum*, indicate a low-latitude pelagic assemblage similar to the one described by Stradner and Steinmetz (1984) from DSDP Site 530 (South Atlantic). The presence of *Micula prinsii* for about 1 m suggests an approximation of the Cretaceous/Tertiary boundary. Yet, on the other hand, the typical increased frequency of *Thoracosphaera* characteristic of the Cretaceous/Tertiary boundary was not observed in Hole 661A.

### Hiatuses

A study of marker species distribution allows recognition of several hiatuses in the Leg 108 sedimentary sequences. In order of increasing age, the first hiatus was observed at Sites 657 and 658 from 0.5 to 1.4 Ma (top CN14 to base CN13b), as a result of slumped deposits corresponding to a mass flow. Along the active transform fault of the Romanche Fracture, Sites 662–663 and 664 show the same hiatus at 1.25 Ma (CN13b), which is due to a major seismic event. Around the Miocene/Pliocene boundary of Site 657 (top CN10b to base CN9a), at the level of lithologic change from red clays to carbonate facies (145 mbsf), a hiatus (4.6–6.0 Ma) is inferred that represents most of the Messinian period.

At Site 667, in the late Miocene, the pelagic deposition was disrupted by a slump creating reworking. It is probable that a middle to upper Miocene hiatus occurs in the interval from upper NN9 to basal NN8 (8.5–10.0 Ma). Another Miocene hiatus representing about 3.5 m.y. was detected in the early Miocene at Site 659, from upper NN3 to basal NN2 (17–21.5 Ma).

The oldest hiatus was registered at Site 661, because the barren interval of coccoliths from the upper Miocene to the Upper Cretaceous is only 23.3 m long (82–105.3 mbsf) and represents over 57 m.y. Thus, it probably contains at least one major hiatus.

### CONCLUSIONS

On Leg 108, in the subtropical upwelling region off the shore of Cap Blanc (Sites 657–659) and in the two sites of the Kane Gap area (Sites 660 and 661), the somewhat undisturbed cores allow a reliable succession of 30 calcareous nannofossil biohorizons from the late Pleistocene to the Oligocene/Miocene boundary (Sites 667 and 659). A direct correlation of nannofossil events with magnetostratigraphy furnishes a good

time control for the Pleistocene and late Pliocene during the last 2 Ma (Fig. 3).

The boundaries between the usual Quaternary geomagnetic epochs were determined at Sites 657, 658, 659, 660, 661, and 665. The best magnetic record in the late Pliocene was found at Sites 657 and 665–660. This last site provides geomagnetic data from the lower Pliocene and the uppermost Miocene till the top of Epoch C4 (6.70 Ma).

The magnetobiochronology derived from paleomagnetic and calcareous nannofossil stratigraphic analyses of Quaternary and Pliocene sedimentary sequences recovered during Leg 108 reveals a correct consistency with DSDP results, set from South Atlantic legs (Stradner and Steinmetz, 1984; Hsü et al., 1984). They are all in reasonable agreement with various data from the literature (Gartner, 1977; Backman and Shackleton, 1983).

#### ACKNOWLEDGMENTS

Comments by J. Baldauf and critical and valuable reviews by K. Perch-Nielsen and an anonymous reviewer significantly improved the manuscript and are greatly appreciated. The study was supported by a grant from ATP ODP France.

#### REFERENCES

- Backman, J., and Shackleton, N. J., 1983. Quantitative biochronology of Pliocene and early Pleistocene calcareous nannofossils from the Atlantic, Indian, and Pacific Oceans. *Mar. Micropaleontol.*, 8:141–170.
- Berggren, W. A., Kent, D. V., and Van Couvering, J. A., 1985. Neogene geochronology and chronostratigraphy. In Snelling, N. J. (Ed.), *The Chronology of the Geologic Record*. Geol. Soc. Mem. (London), 10:211–260.
- Bukry, D., 1973. Low-latitude coccolith biostratigraphic zonation. In Edgar, N. T., Saunders, J. B., et al., *Init. Repts. DSDP*, 15: Washington (U.S. Govt. Printing Office), 685–703.
- , 1985. Mid-Atlantic Ridge coccolith and silicoflagellate biostratigraphy, Deep Sea Drilling Project Sites 558 and 563. In Bougault, H., Cande, S. C., et al., *Init. Repts. DSDP*, 82: Washington (U.S. Govt. Printing Office), 591–603.
- Bukry, D., and Bramlette, M. N., 1970. Coccolith age determinations Leg 3, Deep Sea Drilling Project. In Maxwell, A. E., Von Herzen, R. P., et al., *Init. Repts. DSDP*, 3: Washington (U.S. Govt. Printing Office), 589–611.
- Gartner, S., 1977. Calcareous nannofossil biostratigraphy and revised zonation of the Pleistocene. *Mar. Micropaleontol.*, 2:1–25.
- Gartner, S., Chow, J., and Stanton, R. J., 1987. Late Neogene paleoceanography of the eastern Caribbean, the Gulf of Mexico, and the eastern equatorial Pacific. *Mar. Micropaleontol.*, 12:255–304.
- Hsü, K. J., Percival, S. F., Wright, R. C., and Petersen, N., 1984. Numerical ages of magnetostratigraphically calibrated biostratigraphic zones. In Hsü, K. J., La Brecque, J. L., et al., *Init. Repts. DSDP*, 73: Washington (U.S. Govt. Printing Office), 623–636.
- Manivit, H., 1984. Paleogene and Upper Cretaceous calcareous nannofossils from Deep Sea Drilling Project Leg 74. In Moore, T. C., Rabinowitz, P. D., *Init. Repts. DSDP*, 74: Washington (U.S. Govt. Printing Office), 475–499.
- Martini, E., 1971. Standard Tertiary and Quaternary calcareous nannoplankton zonation. In Farinacci, A. (Ed.), *Proceedings of the II Planktonic Conference, Roma, 1970*: Rome (Ed. Tecno-scienza), 2:739–785.
- Monechi, S., and Thierstein, H. R., 1985. Late Cretaceous–Eocene nannofossil and magnetostratigraphic correlations near Gubbio, Italy. *Mar. Micropaleontol.*, 9:419–440.
- Okada, H., and Bukry, D., 1980. Supplementary modification and introduction of code numbers to the low-latitude coccolith biostratigraphic zonation (Bukry, 1973, 1975). *Mar. Micropaleontol.*, 5:321–325.
- Parker, M. E., Clark, M., and Wise, S. W., Jr., 1985. Calcareous nannofossils of Deep Sea Drilling Project Sites 558 and 563, North Atlantic Ocean: biostratigraphy and the distribution of Oligocene braarudosphaerids. In Bougault, H., Cande, S. C., et al., *Init. Repts. DSDP*, 82: Washington (U.S. Govt. Printing Office), 559–589.
- Perch-Nielsen, K., 1977. Albian to Pleistocene calcareous nannofossils from the western south Atlantic, Deep Sea Drilling Project 39. In Supko, P. R., Perch-Nielsen, K., et al., *Init. Repts. DSDP*, 39: Washington (U.S. Govt. Printing Office), 699–823.
- Pflaumann, U., and Čepek, P., 1982. Cretaceous foraminiferal and nannoplankton biostratigraphy and paleoecology along the West African Continental Margin. In von Rad, U., Hinz, K., Sarthein, M., and Siebold, E. (Eds.), *Geology of the Northwest African Continental Margin*: Berlin-Heidelberg-New York (Springer-Verlag), 309–353.
- Roth, P. H., and Thierstein, H. R., 1972. Calcareous nannoplankton: Leg 14 of the Deep Sea Drilling Project. In Hayes, D. E., Pimm, A. C., et al., *Init. Repts. DSDP*, 14: Washington (U.S. Govt. Printing Office), 421–485.
- Stradner, H., and Steinmetz, J., 1984. Cretaceous calcareous nannofossils from the Angola Basin, Deep Sea Drilling Project Site 530. In Hay, W. W., Sibuet, J.-C., et al., *Init. Repts. DSDP*, 75: Washington (U.S. Govt. Printing Office), 565–649.
- Thierstein, H. R., 1976. Mesozoic calcareous nannoplankton biostratigraphy of marine sediments. *Mar. Micropaleontol.*, 1:325–362.
- Thierstein, H. R., Geitzenauer, K. R., Molino, B., and Shackleton, N. J., 1977. Global synchronicity of late Quaternary coccolith datum levels: validation by isotopes. *Geology*, 5:400–404.

Date of initial receipt: 24 May 1988

Date of acceptance: 13 January 1989

Ms 108B-126

#### APPENDIX

##### CENOZOIC CALCAREOUS NANNOFOSSILS CONSIDERED IN THIS CHAPTER (in alphabetical order by species epithets)

- Sphenolithus abies* Deflandre, 1954. This taxon is grouped with *Sphenolithus neoabies* under the name *Sphenolithus* spp.
- Cyclarcolithus abiseptus* (Müller, 1970) Bukry, 1973
- Ceratolithus acutus* Gartner and Bukry, 1975
- Discoaster adametus* Bramlette and Wilcoxon, 1967
- Helicosphaera ampliaperta* Bramlette and Wilcoxon, 1967
- Amaurolithus amplificus* (Bukry and Percival, 1971) Gartner and Bukry, 1975
- Oolithus antillarum* (Cohen, 1964) Reinhardt, 1968
- Discoaster asymmetricus* Gartner, 1969
- Dictyococcites bisectus* (Hay et al., 1966) Bukry and Percival, 1971
- Sphenolithus belemnos* Bramlette and Wilcoxon, 1967
- Discoaster bellus* Bukry and Percival, 1971
- Discoaster berggrenii* Bukry, 1971
- Discoaster bollii* Martini and Bramlette, 1963
- Discoaster brouweri* Tan Sin Hok, 1927
- Discoaster calcaris* Gartner, 1967
- Catinaster calyculus* Martini and Bramlette, 1963
- Gephyrocapsa carribeanica* Boudreux and Hay, 1967
- Triquetrorhabdulus carinatus* Martini, 1965
- Discoaster challengeri* Bramlette and Riedel, 1954
- Sphenolithus ciperoensis* Bramlette and Wilcoxon, 1967
- Rhabdosphaera clavigera* Murray and Blackman, 1898
- Catinaster coalitus* Martini and Bramlette, 1963
- Helicosphaera compacta* Bramlette and Wilcoxon, 1967
- Sphenolithus conicus* Bukry, 1971a
- Ceratolithus cristatus* Kamptner, 1954
- Reticulofenestra daviesi* (Haq, 1968) Haq, 1971
- Discoaster deflandrei* Bramlette and Riedel, 1954
- Amaurolithus delicatus* Gartner and Bukry, 1975
- Sphenolithus dissimilis* Bukry and Percival, 1971
- Sphenolithus distentus* (Martini, 1965) Bramlette and Wilcoxon, 1967
- Crenalithus doronicoides* (Black and Barnes, 1961) Roth, 1973. This taxon is used broadly and includes *Coccolithus productus* (Kamptner) Sachs and Skinner, 1973; *Crenalithus productellus* Bukry, 1975; and other small coccoliths with no discernible bridge.
- Discoaster druggii* Bramlette and Wilcoxon, 1967
- Helicosphaera euphratis* Haq, 1966
- Discoaster exilis* Martini and Bramlette, 1963

*Ericsonia fenestrata* (Deflandre and Fert, 1954) Stradner, 1968  
*Cyclacolithus floridanus* (Roth and Hay, 1967) Bukry, 1971  
*Gephyrocapsa* spp. (small). This grouping includes *Gephyrocapsa aperta* Kamptner, 1963; *Gephyrocapsa ericsonii* McIntyre and Bé; *Gephyrocapsa kamptneri* Deflandre and Fert, 1954; and *Gephyrocapsa protohuxleyi* McIntyre, 1970. All these species cannot be separated with the light microscope.  
*Helicosphaera granulata* Bukry and Percival, 1971  
*Reticulofenestra gartneri* Roth and Hay, 1971  
*Discoaster hamatus* Martini and Bramlette, 1963  
*Sphenolithus heteromorphus* Deflandre, 1953  
*Syracosphaera histrica* Kamptner, 1941  
*Emiliania huxleyi* (Lohmann, 1902) Hay and Mohler, 1967  
*Discoaster intercalaris* Bukry, 1971  
*Helicosphaera intermedia* Deflandre, 1942  
*Discolithina japonica* Takayama, 1967  
*Helicosphaera kamptneri* Hay and Mohler, 1967  
*Discoaster kugleri* Martini and Bramlette, 1963  
*Pseudoemiliana lacunosa* (Kamptner, 1963) Gartner 1969c  
*Calcidiscus leptoporus* (Murray and Blackman, 1898) Loeblich and Tappan, 1978  
*Discoaster loeblichii* Bukry, 1971  
*Calcidiscus macintyrei* (Bukry and Bramlette, 1969) Loeblich and Tappan, 1978  
*Triquetrorhabdulus milowii* Bukry, 1971  
*Coccolithus miopelagicus* Bukry, 1971  
*Umbilicosphaera mirabilis* Lohmann, 1902  
*Sphenolithus moriformis* (Brönnimann and Stradner, 1960) Bramlette and Wilcoxon, 1967  
*Sphenolithus neoabies* Bukry and Bramlette, 1969  
*Discoaster neohamatus* Bukry and Bramlette, 1969  
*Discoaster neorectus* Bukry, 1971  
*Coronocyclus nitescens* (Kamptner, 1964)  
*Helicosphaera obliqua* Bramlette and Wilcoxon, 1967  
*Gephyrocapsa oceanica* Kamptner, 1943  
*Coccolithus pelagicus* (Wallich, 1977) Schiller, 1930  
*Discoaster pentaradiatus* Tan Sin Hok, 1927  
*Hayaster perplexus* (Bramlette and Riedel, 1954) Bukry, 1973  
*Sphenolithus predistinctus* Bramlette and Wilcoxon, 1967  
*Discoaster prepentaradiatus* Bukry and Percival, 1971  
*Amaurolithus primus* (Bukry and Bramlette, 1971) Gartner and Bukry, 1975  
*Reticulofenestra pseudoumbilica* (Gartner, 1967) Gartner, 1969  
*Discoaster pseudovariabilis* Martini and Worsley, 1971  
*Syphosphaera pulcherrima* Deflandre, 1942  
*Syracosphaera pulchra* Lohmann, 1902  
*Discoaster quinqueramus* Gartner, 1969  
 Small *Reticulofenestra* spp. is a group of diverse *Reticulofenestra* that includes such small forms as *R. minuta* Roth and *R. minutula* (Gartner) et *R. haqii* Backman.  
*Geminolithella rotula* (Kamptner, 1956) Backman, 1980  
*Ceratolithus rugosus* Bukry and Bramlette, 1968  
*Triquetrorhabdulus rugosus* Bramlette and Wilcoxon, 1967  
*Helicosphaera sellii* (Bukry and Bramlette, 1969) Jafar and Martini, 1975  
*Orthorhabdus serratus* Bramlette and Wilcoxon, 1967  
*Umbilicosphaera sibogae* (Weber-van-Bosse, 1901) Gaarder, 1970

*Thoracosphaera* sp.  
*Discoaster surculus* Martini and Bramlette, 1963  
*Pontosphaera syracusana* Lohmann, 1902  
*Discoaster tamalis* Kamptner, 1967  
*Ceratolithus telesmus* Norris, 1975  
*Amaurolithus tricorniculatus* (Gartner, 1967) Gartner and Bukry, 1975  
*Discoaster triradiatus* Tan Sin Hok, 1927  
*Discoaster variabilis* Martini and Bramlette, 1963  
*Helicosphaera truemppi* Biolzi and Perch-Nielsen (1982)

CRETACEOUS SPECIES AT SITE 661

*Ceratolithus aculeus* (Stradner, 1961) Prins and Sissingh, 1977  
*Rhagodiscus angustus* (Stradner, 1963) Reinhardt, 1971  
*Reinhardtites anthophorus* (Deflandre, 1959) Wise and Wind, 1976  
*Watznaueria barnesae* (Black, 1959) Perch-Nielsen, 1968  
*Lithraphidites carniolensis* Deflandre, 1963  
*Micula concava* (Stradner, 1960) Verbeek, 1976  
*Biscutum constans* (Gorka, 1957) Black, 1959  
*Cretarhabdus crenulatus* Bramlette and Martini, 1964; emend. Thierstein, 1971  
*Prediscosphaera cretacea* (Arkhangelsky, 1912) Gartner, 1968  
*Arkhangelskiella cymbiformis* Vekshina, 1959  
*Microrhabdulus decoratus* Deflandre, 1959  
*Tetrapodorhabdus decorus* (Deflandre and Fert, 1954) Wind and Wise, 1976  
*Cribrosphaerella diplogrammus* (Deflandre, 1954) Reinhardt, 1964  
*Zeugrhabdus embergeri* (Noel, 1959) Stradner, 1963 n.  
*Cribrosphaerella ehrenbergii* (Arkhangelsky, 1912) Deflandre, 1952  
*Broinsonia enormis* (Shumenko, 1968) Manivit, 1971  
*Eiffellithus eximius* (Stover, 1966) Perch-Nielsen, 1968  
*Crirocorma gallica* (Stradner, 1963) Bramlette and Martini, 1964  
*Quadrum gothicum* (Deflandre, 1959) Prins and Perch-Nielsen, 1977  
*Prediscosphaera grandis* Perch-Nielsen, 1979  
*Ceratolithoides kamptneri* Bramlette and Martini, 1964  
*Reinhardtites levius* Prins and Sissingh, 1977  
*Chiastozygus litterarius* (Gorka, 1957) Manivit, 1971  
*Kamptnerius magnificus* Deflandre, 1959  
*Prediscosphaera majungae* Perch-Nielsen, 1973  
*Micula murus* (Martini, 1961) Bukry, 1973  
*Calculites obscurus* (Deflandre) Prins and Sissingh, 1977  
*Ahmuellerella octoradiata* (Gorka, 1957) Reinhardt, 1966  
*Tranolithus orionatus* Stover, 1966  
*Manivitella pemmatoides* (Deflandre, 1965) Thierstein, 1971  
*Micula praemurus* (Bukry, 1973) Stradner and Steinmetz, 1984  
*Micula prinsii* Perch-Nielsen, 1979  
*Cylindricalithus serratus* Bramlette and Martini, 1964  
*Quadrum sissinghii* Perch-Nielsen, 1985  
*Prediscosphaera spinosa* Bramlette and Martini, 1964  
*Zygodiscus spiralis* Bramlette and Martini, 1964  
*Micula staurophora* (Gardet, 1955) Stradner, 1963  
*Microrhabdulus stradneri* Bramlette and Martini, 1964  
*Cretarhabdus surirellus* (Deflandre) Reinhardt, 1970  
*Micula swastica* (Prins, 1977) Stradner and Steinmetz, 1984  
*Quadrum trifidum* (Stradner, 1961) Prins and Perch-Nielsen, 1977  
*Eiffellithus turriseiffeli* (Deflandre and Fert, 1954) Reinhardt, 1965  
*Thoracosphaera cf. deflandrei* Kamptner, 1956

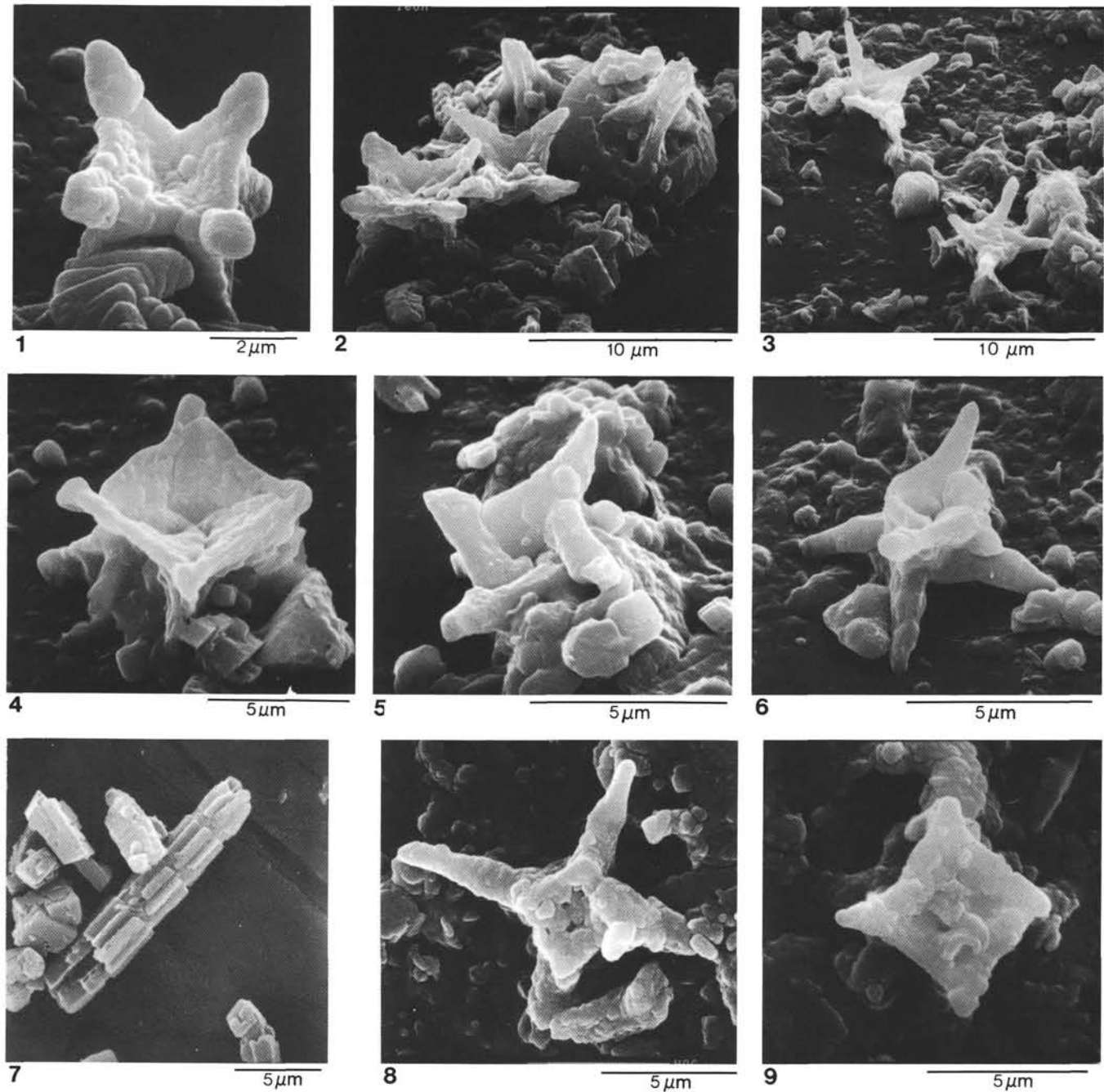


Plate 1. All samples from Plates 1–4 were observed with a scanning electron microscope. The samples are Maestrichtian in age. The magnification of each picture can be calculated from the scale bar. 1. *Micula prinsii* Perch-Nielsen. Oblique proximal view with overgrown ends: Sample 108-661A-12H-6, 122 cm. 2, 3. *Micula concava* (Stradner) Verbeek. (2) Assemblage of *Micula concava* and *Prediscosphaera grandis*. (3) Proximal view: Sample 108-661A-13H-1, 100 cm. 4. *Micula swastica* (Prins) Stradner and Steinmetz. Plane view: Section 108-661A-13H-CC. 5. *Micula murus* (Martini) Bukry. Plane view: Sample 108-661A-13H-1, 100 cm. 6, 9. *Micula staurophora* (Gardet) Stradner. (6) Oblique side view. (9) Plane view: Sample 108-661-18H-2, 100 cm. 7. *Microrhabdulus stradneri* Bramlette and Martini, Sample 108-661A-18H-2, 100 cm. 8. *Quadrum sissinghii* Perch-Nielsen. Proximal view: Section 108-661A-16X-CC.

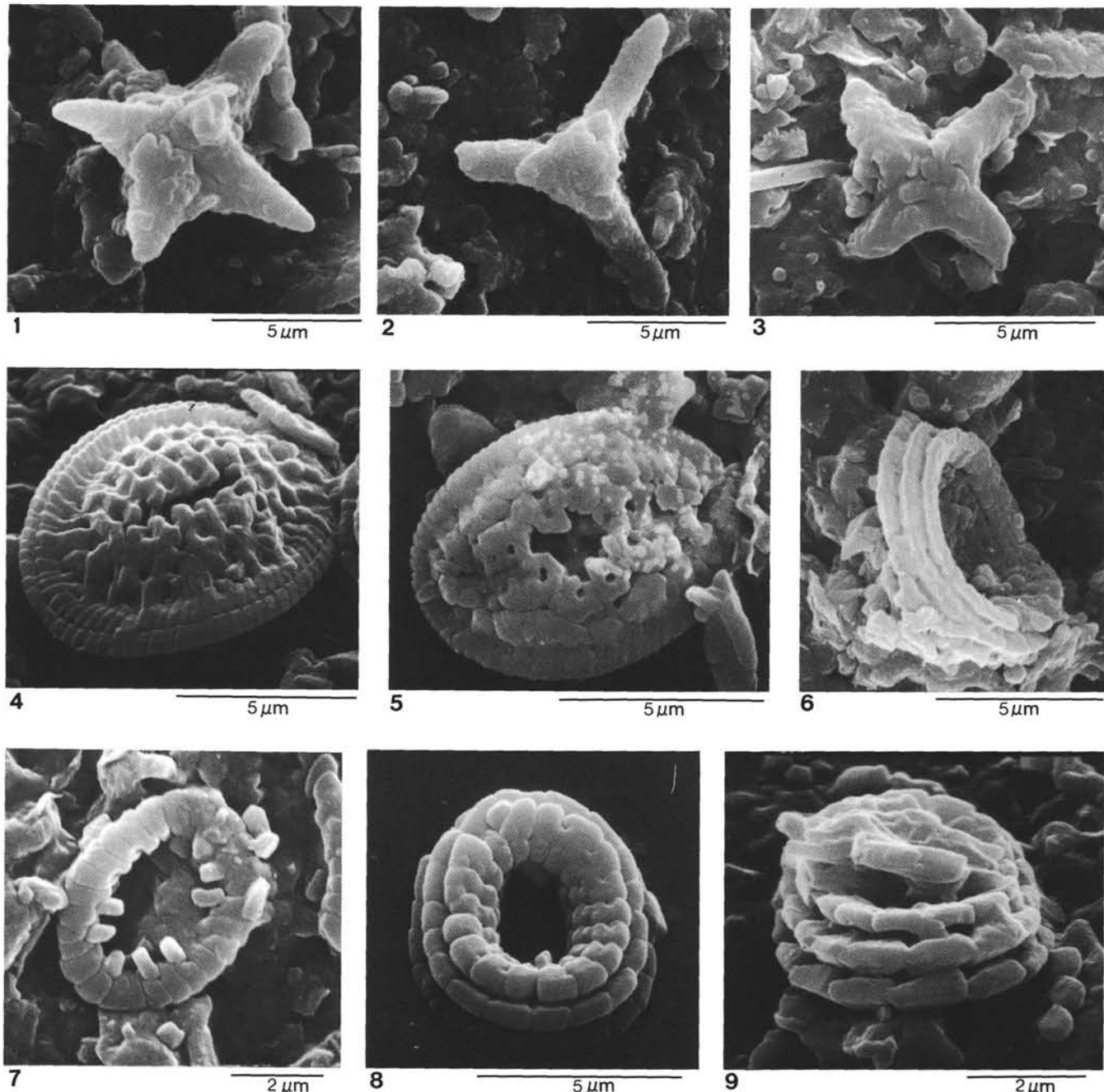


Plate 2. 1, 3. *Quadrum gothicum* (Deflandre) Prins and Perch-Nielsen. (1) Plane view. (3) Overgrown specimen: Section 108-661A-16X-CC. 2. *Quadrum trifidum* (Stradner) Prins and Perch-Nielsen. Slender specimen on distal view: Section 108-661A-16X-CC. 4, 5. *Arkhangelskiella cymbiformis* Vekshina. (4) Distal view of preserved specimen. (5) Distal view of etched specimen: Section 108-661A-13H-CC. 6, 8, 9. *Cribrosphaerella ehrenbergii* (Arkhangelskij) Deflandre. (6) Lateral view of overgrown specimen: Section 108-661A-13H-CC. (8) Proximal view with dissolved central area: Sample 108-661A-12H-6, 122 cm. (9) Proximal view of etched specimen: Section 108-661A-13H-CC. 7. *Cretarhabdus cf. surrirellus* (Deflandre), Reinhardt. Distal view: Sample 108-661A-12H-6, 122 cm.

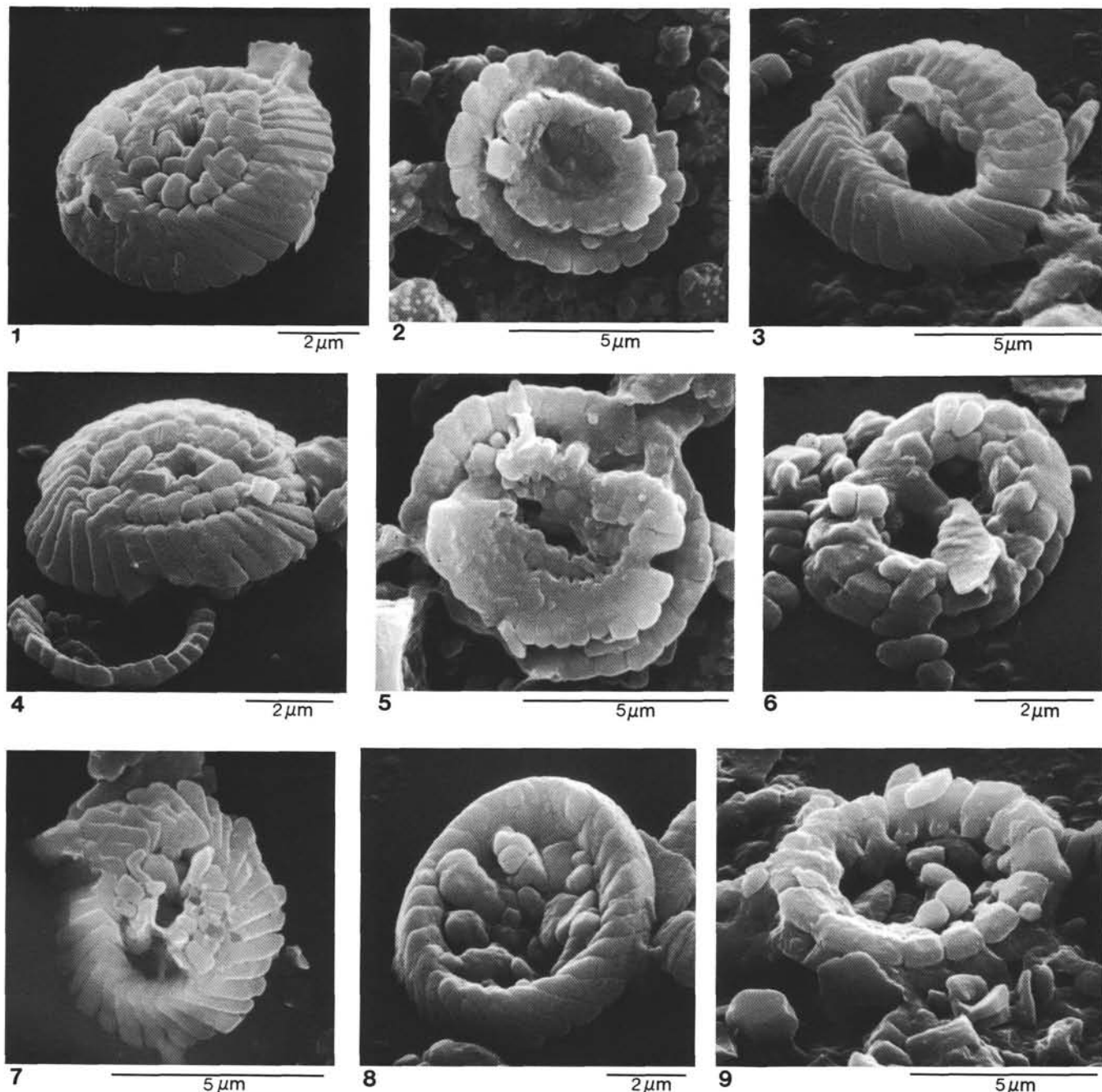


Plate 3. 1, 2, 4, 5, 7. *Watznaueria barnesae* (Black) Perch-Nielsen. Distal view with different preservation state. (1, 4) Section 108-661A-13H-CC. (7) Sample 108-661A-12H-6, 122 cm. (2, 5) Proximal view of badly preserved specimens: Sample 108-661A-13H-1, 100 cm. 3, 6, 9. *Zygodiscus* cf. *spiralis* Bramlette and Martini. (3) Distal view: Sample 108-661A-13H-1, 100 cm. (6, 9) Proximal view of overgrown and etched specimens: Section 108-661A-13H-CC. 8. *Eiffelithus turriseiffeli* Deflandre and Fert. Proximal view of overgrown specimen: Section 108-661A-13H-CC.

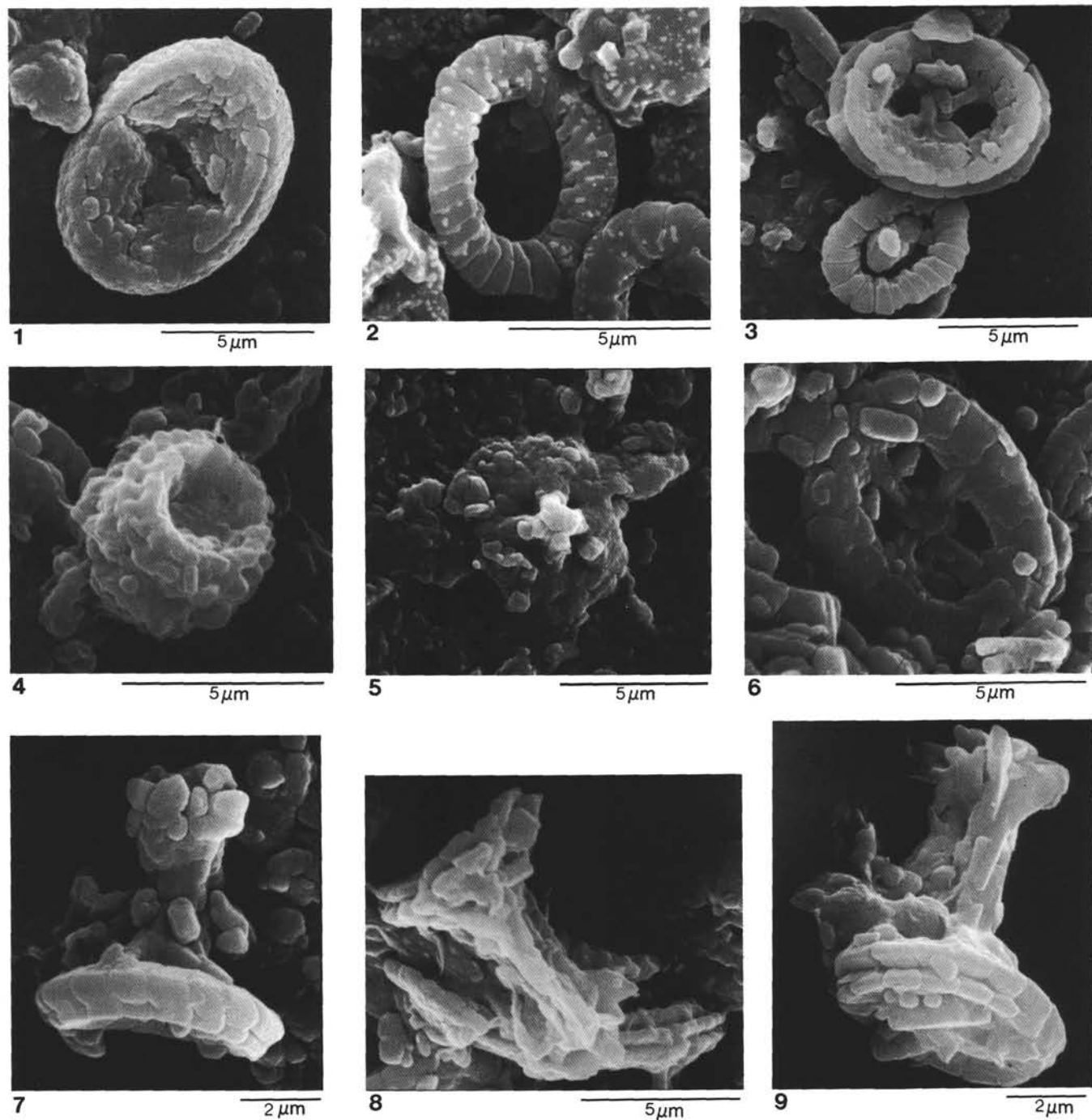


Plate 4. 1. *Reinhardtites levis* Prins and Sissingh. Proximal view: Section 108-661A-16X-CC. 2. *Manivitella* cf. *pemmatoides* (Deflandre) Theirstein. Plane view of distal side: Sample 108-661A-13H-1, 100 cm. 3. *Chiastozygus litterarius* (Gorka) Manivit. Proximal view: Section 108-661A-16X-CC. 4. *Cribrocorona gallica* (Stradner) Bramlette and Martini. Oblique lateral view: Sample 108-661A-13H-1, 100 cm. 5, 9. *Prediscosphaera cretacea* (Arkhangelsky) Gartner. (5) Distal view of recrystallized basal plate. (9) Lateral view of complete coccolith: Section 108-661A-16X-CC. 6. *Prediscosphaera spinosa* Bramlette and Martini. Proximal view: Sample 108-661A-13H-1, 100 cm. 7, 8. *Prediscosphaera* cf. *majungae* Perch-Nielsen. (7) Lateral view of overgrown coccolith. (8) Lateral view of a specimen intermediary between *P. majungae* and *P. cretacea*: Sample 108-661A-13H-1, 100 cm.